

## RESEARCH ARTICLE OPEN ACCESS

# From Archives to Insights: Extreme Weather Events and Socio-Economic Impacts in Madagascar From Newly Digitised Historical Climate Records (1949–1966)

Simon Noone<sup>1</sup>  | Caoilfhionn D'Arcy<sup>2</sup>  | Kevin Healion<sup>1</sup> | Peter Thorne<sup>1</sup> 

<sup>1</sup>Irish Climate Analysis and Research UnitS (ICARUS), Department of Geography, Maynooth University, Maynooth, Ireland | <sup>2</sup>Department of Geography, Maynooth University, Maynooth, Ireland

**Correspondence:** Simon Noone ([simon.noone@mu.ie](mailto:simon.noone@mu.ie))

**Received:** 22 August 2025 | **Revised:** 20 October 2025 | **Accepted:** 17 November 2025

**Keywords:** Africa | climate data rescue | cyclones | extreme weather | Madagascar | meteorological observations

## ABSTRACT

Billions of historical weather observations dating back centuries remain in the original paper form, vulnerable to permanent loss due to deterioration and unusable by modern science. Africa, in particular, faces significant challenges in climate impact research due to the scarcity of consistent, high-quality historical observational data. The Climate Data Rescue-Africa (CliDaR-Africa) project engages second-year undergraduates at Maynooth University, Ireland, in participatory, classroom-based digitization of unique African meteorological records. This paper presents detailed outcomes from the CliDaR-Africa projects during 2023 and 2024 which successfully digitised over 300,000 unique sub-daily and daily meteorological observations from stations in Madagascar and the Central African Republic spanning 1949 to 1966. Initial analysis of the rescued Madagascar records reveals several notable extreme weather events, underscoring the country's high vulnerability to hazards such as hot spells, droughts, heavy rainfall, and particularly tropical cyclones. Among these is a sequence of tropical cyclones which received limited international coverage either at the time or in the intervening years. By bringing these overlooked extremes to light, the data potentially alters our understanding of extremes and their unusualness in the modern era. Complementary documentary evidence corroborates the meteorological findings and provides rare, detailed insights into the socio-economic consequences, illustrating how these extremes impacted on the communities and economies of Madagascar at the time.

## 1 | Introduction

Most existing digitised climate data primarily consist of records from the mid-20th century onward (Chimani et al. 2022; Noone et al. 2021; Brönnimann et al. 2018; WMO 2016; Brunet and Jones 2011; Allan et al. 2011). Prior to this period, many of the digitally available station records are of poor quality, incomplete or have a limited range of observed variables (Noone et al. 2021; Cram et al. 2015; Rennie et al. 2014; Schneider et al. 2013). Yet, billions of weather observations dating back centuries remain in paper form, vulnerable to decay and potential loss (Brönnimann et al. 2019). The recovery, digitization, quality assurance and

effective use of long historical, high-quality meteorological records are essential for contextualising recent climate variability, identifying emerging trends, and ground-truthing future climate models (Luterbacher et al. 2024; Brunet et al. 2013). Sir Winston Churchill once said ‘The farther backward you can look, the farther forward you are likely to see’ (Churchill n.d.).

Increasing the amount of historical climate data, especially in data sparse regions, will also allow studies to identify and analyse past extreme weather events such as storms, droughts and heatwaves (Craig and Hawkins 2024; Luterbacher et al. 2024; Hawkins, Brohan, et al. 2023; Murphy et al. 2023; Dooley

This is an open access article under the terms of the [Creative Commons Attribution](https://creativecommons.org/licenses/by/4.0/) License, which permits use, distribution and reproduction in any medium, provided the original work is properly cited.

© 2025 The Author(s). *International Journal of Climatology* published by John Wiley & Sons Ltd on behalf of Royal Meteorological Society.

et al. 2023; Noone et al. 2017). Such analyses provide invaluable insights into the frequency, intensity, and patterns of past climatic anomalies, providing a better understanding of long-term climate variability.

Due to an absence of sufficient historical data, the Intergovernmental Panel on Climate Change (IPCC) AR6 Working Group I (AR6 WGI) was unable to comprehensively assess climate extremes in several regions, hindering the validation of future climate extreme projections and limiting effective adaptation planning (Trisos et al. 2022; Seneviratne et al. 2021). Africa is one of these regions, where climate impact research is limited and more reliable historical climate data is urgently needed (Kaspar et al. 2022; Dinku 2019).

Historical data is also important for the production of reanalysis datasets. Availability of more data can help produce more reliable representations of past weather (Copernicus Climate Change Service 2024; Hawkins, Brohan, et al. 2023; Slivinski et al. 2019). Brönnimann (2022) demonstrated that incorporating more ship historical observations into the 'Twentieth Century Reanalysis' Version 3 improved reanalysis output quality across parts of Sub Saharan African (Slivinski et al. 2019). The European Centre for Medium Range Weather Forecasts (ECMWF) is also continuing to promote the acquisition and use of historical observations in their reanalysis datasets, especially data sparse regions such as Africa (Hersbach 2023).

Despite extensive global climate data rescue efforts conducted by diverse contributors requiring significant financial and human resources (e.g., Engström et al. 2023; Hawkins, Burt, et al. 2023; Lakkis et al. 2023; Hawkins et al. 2019; Ashcroft et al. 2018; Ryan et al. 2018; Noone et al. 2015; Kaspar et al. 2015; Wilkinson et al. 2011), a very substantial amount of historical climate data still remains in archives and needs to be digitised.

A key potential source over Africa, but by no means the only source, is a collection of data that were imaged to microfiche and microfilm in the late 1980s/early 1990s at African Center of Meteorological Applications for Development (ACMAD) in association with the Belgian meteorological service (RMI) and the World Meteorological Organization (WMO). The majority of sub-Saharan countries took part in this initiative providing many or all of their historical records for imaging. For a long time these data were feared lost, rendered unusable by their storage on what turned out to be unstable media. In recent years a copy, kept in a glass fronted airtight cabinet was found at RMI and the films and fiche were imaged under contract to the Copernicus Climate Change Service resulting in some 4–5 million recovered images of original records. These images now reside in electronic format failsafe saved at several locations.

In 2022, the EU funded 'Copernicus C3S2-311 Lot 1 Collection and Processing of In Situ Observations' contract (Noone et al. 2021) led by the ICARUS Climate Research Centre at Maynooth University (MU) in Ireland began to address the challenge of converting the saved images to digital data records. The C3S2-311 team along with the MU Geography department designed the Climate Data Rescue Africa Project (CliDaR-Africa). The project engaged second-year undergraduate students to digitise historical meteorological data from scanned images in

the ACMAD data collection (Noone et al. 2024). Due to its success, the CliDaR-Africa project was rolled out again with MU students in 2023 and 2024.

This paper will present the data digitization efforts completed by students at MU in the CliDaR-Africa projects during 2023 and 2024. To illustrate the utility and significance of this data, this paper presents the findings of an initial analysis highlighting several notable extreme weather events identified in the recently digitised meteorological records from Madagascar. Open access online documentary evidence is then used to validate some of the findings and offer valuable insights into their socio-economic impacts.

The remainder of this paper is organised as follows: Section 2 introduces the main study area and outlines the data selected for digitization. Section 3 details the methods employed for data digitization, quality control, and subsequent analysis. Section 4 presents the results of the analysis. Section 5 discusses potential future work and data availability, while Section 6 concludes the paper with final remarks.

## 2 | Main Study Area

Madagascar is a former French colony with a climate that is varied, with specific different microclimates due to its geographical position in the South-Western Indian Ocean and varying topography. However, Madagascar's climate is predominantly tropical, characterised by a hot and rainy season from November to April and a cooler, drier season from May to October. Regional variations include a humid eastern coast, drier central highlands, and arid southern areas (Goodman et al. 2003; Tadross et al. 2008). The country is highly vulnerable to climate change, experiencing increasing temperatures, unpredictable rainfall, drought and more frequent extreme weather events (Hannah et al. 2008). Future shifts in climate are expected to exacerbate environmental challenges and affect agricultural productivity, biodiversity and food security (Harvey et al. 2014). Madagascar is abundant in natural resources and biodiversity but struggles with high poverty, food insecurity, rapid population growth and resource exploitation (Weiskopf et al. 2021).

Madagascar is located in one of the most active regions in the world for tropical cyclones. Cyclones that make landfall can result in significant socio-economic impacts, including major damage to infrastructure and loss of life (Khan et al. 2025; Serele et al. 2023; Nash et al. 2015). Between 2002 and 2023 75 cyclones passed close to or made direct landfall on Madagascar (Khan et al. 2025). The strength of these cyclones over this period varied from Saffir-Simpson scale Category 1 that has wind speeds of 119–153 km/h up to Category 5 with wind speeds of 252 km/h or higher (Khan et al. 2025; National Hurricane Center 2019). Some of these cyclones were particularly noteworthy, causing severe damage and loss of life across Madagascar (Serele et al. 2023). Cyclone Batsirai in 2022, was a Category 4 cyclone with a maximum sustained wind-speed of 230 km/h, and a lowest central pressure of 932.0 hPa (Khan et al. 2025). Category 5 Freddy in 2023 is the most long-lived tropical cyclone ever recorded, lasting over 35 days with sustained wind speeds over 255 km/h. Notably Freddy had a rainband diameter of 700–1000 km

and made landfall multiple times, causing over 1400 deaths and damage costing in excess of \$655 million (Trewin et al. 2024; Liu et al. 2023).

Moreover, the people who live in the southern semi-arid and arid areas of Madagascar, known as the 'Deep South' have experienced so many frequent natural disasters that they have named the after-effects from such events; 'Kere' (Ralaingita et al. 2022). 'Kere' is a repeated devastating famine that studies suggest is caused by not only extreme weather events such as drought, but by many interacting factors, including deforestation, pests, disease, poverty and other social issues (Ralaingita et al. 2022). This regular cycle of events results in thousands of deaths annually and perpetuates ongoing poverty in the two main southern regions of Androy and Atsimo-Andrefana which cover an area of roughly 50,000 km<sup>2</sup>. In recent decades, the people of Madagascar's "Deep South" have experienced a 'Kere' event every single year without exception (Ralaingita et al. 2022).

## 2.1 | Data

For the 2023 and 2024 follow-on CliDaR-Africa projects, unique good quality data images from the ACMAD collection were selected for digitization from five stations in Madagascar and two stations in the Central African Republic (CAR). Table 1 and Figure 1 provide detailed information about each station.

The C3S2-311 team identified Madagascar and CAR images in the ACMAD collection as having unique undigitized data by comparing the data inventories with existing digitised data currently held in existing global sources (Noone et al. 2024). Most of the existing available digitised data for Madagascar only begins

in 1970's with the majority of data prior to this period containing many temporal inconsistencies with only a limited number of variables, specifically just daily observations of temperature and precipitation (Randriamarolaza et al. 2022). The CAR only has 13 stations with existing sub-daily data and this data also has inconsistent temporal and variable coverage.

## 3 | Methods

### 3.1 | Data Digitising and Initial Quality Checks

The C3S2-311 team collaborated with the MU Geography teaching team to update the teaching materials and prepare the data images for distribution to the students in the CliDaR-Africa projects during 2023 and 2024. There were 184 MU students enrolled in the 2023 class and 180 in the 2024 class. Both Madagascar and CAR are former French territories and were using the same logbooks provided from France to record their observations at that time. The data images consisted of three separate sheets for each month of observations, with station name, month and year on each sheet. The observations were recorded at some combination of three times a day and at once a day intervals depending upon observed parameter (see example in Figure 2). The first sheet contains precipitation and evaporation observations, the second sheet contain temperature, cloud and humidity observations and the third sheet has pressure and wind observations.

The C3S2-311 team developed Excel template sheets for the first project in 2022, designed to specifically match the layout of cells in each of the three data image form types (see Figure 3). Form Type 1 Excel template, shown on the left of

**TABLE 1** | Details of all stations selected for digitising in follow on CliDaR-Africa project in 2023 and 2024.

Station name	Country	Latitude, longitude, elevation	Data years for digitising
Ambodifotatra	Madagascar	−16.99, 49.85, 10 m	1955–1960
Nosy Varika	Madagascar	−20.58, 48.53, 10 m	1951–1964
Andapa	Madagascar	−14.39, 49.37, 470 m	1955–1956, 1959–1960
Morombe	Madagascar	−21.75, 43,367, 4 m	1950–1952
Moramanga	Madagascar	−18.95, 48,22, 980 m	1963–1966
Bambari	Central African Republic	5.85, 20.65, 475 m	1953–1956
Birao	Central African Republic	10.28, 22.78, 464 m	1951–1954

Note: Andapa data was selected to fill in some gaps originating from the 2022 project.

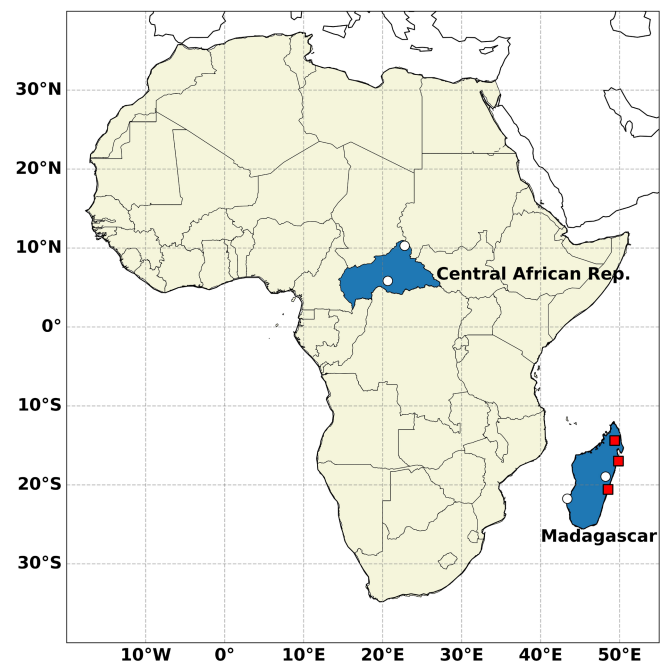


**FIGURE 1** | The location of stations in Madagascar and Central African Republic chosen for digitization in the current CliDaR activities described herein. The three stations denoted by red squares, Ambodifotatra, Nosy Varika and Andapa are focused upon for further analysis and discussion. [Colour figure can be viewed at [wileyonlinelibrary.com](https://onlinelibrary.wiley.com/doi/10.1002/joc.70203)]



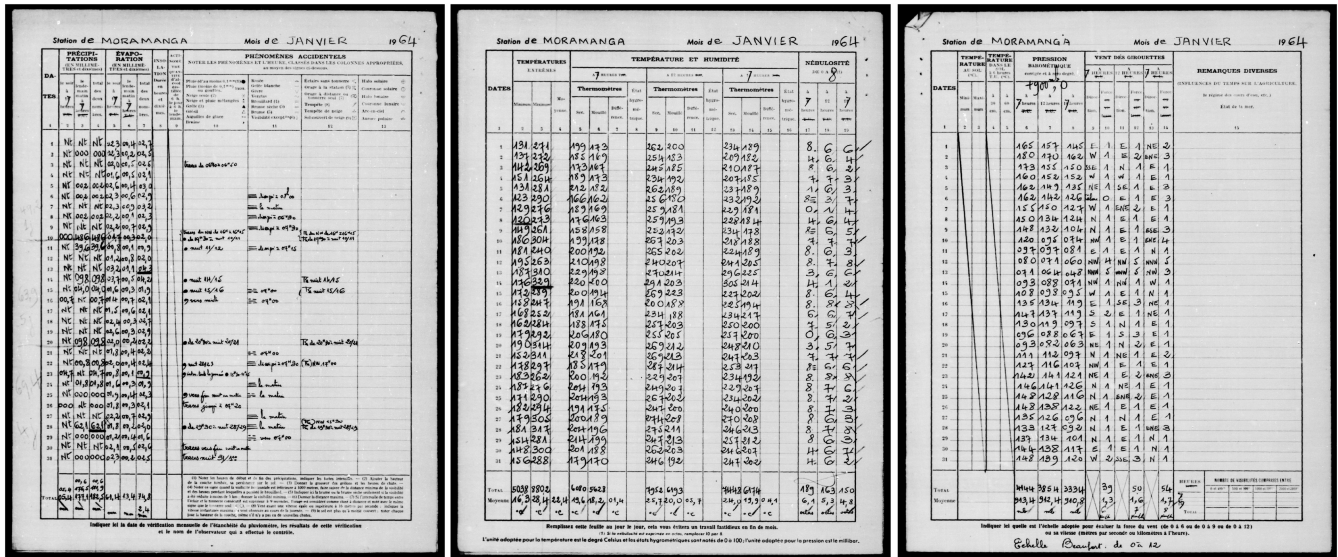


**FIGURE 2** | Example of the three form types for 1 month of data during January 1964 at Moramanga, Madagascar. The first sheet on the left contains precipitation and evaporation observations (accumulations recorded twice daily at 5 PM and 7 AM, with daily totals), the middle sheet contains temperature, cloud and humidity observations (recorded instantaneous values three times daily at 7 AM, 12 noon and 5 PM with daily maximum and minimum temperature recorded once daily) and the sheet on the right contains pressure and wind observations (recorded instantaneous values three times daily at 7 AM, 12 noon and 5 PM).

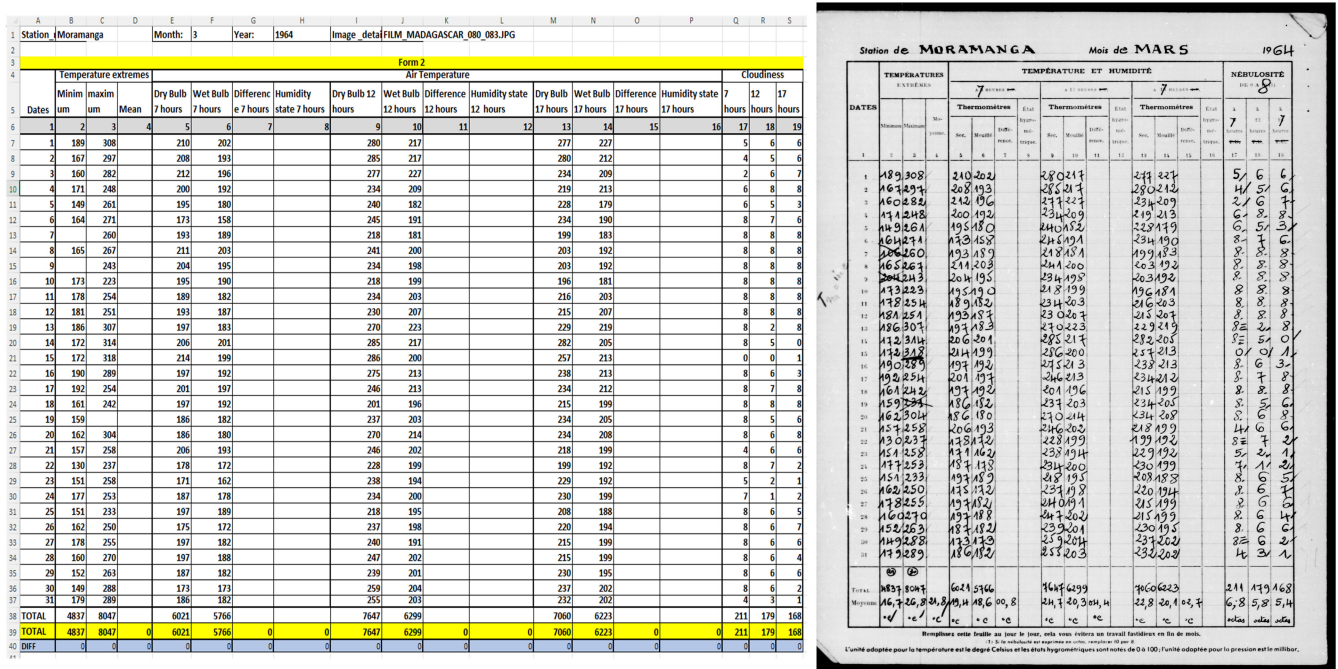


**FIGURE 3** | An example of the completed excel template form that students used to enter the values from the data image sheet. [Colour figure can be viewed at [wileyonlinelibrary.com](https://onlinelibrary.wiley.com)]

Figure 3, was created for data image sheets containing precipitation and evaporation observations. These consist of accumulations recorded twice daily at 7 AM and 5 PM along with daily totals. Form Type 2, corresponding to the middle data image sheet, contains temperature, cloud, and humidity observations. Instantaneous values are recorded three times daily at 7 AM, 12 noon and 5 PM, with daily maximum and minimum temperatures recorded once per day. Form Type 3, shown on the right in Figure 3, contains pressure and wind

observations, recorded as instantaneous values three times daily at 7 AM, 12 noon and 5 PM. As with the first CliDaR-Africa project (Noone et al. 2024), the students were tasked with entering the data exactly as it appeared in the images into the corresponding cells in the templates. Each data sheet column included a total of the entered values at the end, which served as an initial quality check. Students verified the totals using pre-set formulas; if a discrepancy arose, they reviewed the entered data for that column. All non-fixable discrepancies



were documented in a separate notes file, including details of the image and a description of the issue for further review by the C3S2-311 team. Each student was only tasked with digitising 2 months of data which equated to six image sheets of observations in total. This allocation ensured that students were not overwhelmed with keying in too many observations.

In the 2023 CliDaR-Africa project, it was decided to have the students key the data sheets only once to increase throughput. However, upon receiving the completed forms, the C3S2-311 team found that it took much longer to check, verify, and correct errors because each sheet had to be carefully manually checked. Consequently, the team reverted to double keying for the 2024 project. In this approach, half of the students keyed one set of images, while the other half keyed a matching set. This redundancy enabled the C3S2-311 team to use Python programming language (Python Software Foundation 2023) scripts that compared the two sets of keyed data files and flagged any value mismatches. Five stations rescued in 2025; Morombe, Moramanga, Bambari, Birao and Nosy Varik were checked for discrepancies using the mismatch Python code. The C3S2-311 team then cross-checked these flagged values against the original images to resolve potential errors. The mismatched output text files provided the C3S2-311 team with the filename, the row and column where the mismatch occurs, the variable name and the values entered in both sheets. While we cannot guarantee two students did not incorrectly key a value the blind nature of sheet assignment means collusion to deliberately key false values is highly unlikely. In addition, since students are distributed across seven–eight different classes, every effort was made to avoid assigning the same set of data image sheets within a single class. Although not foolproof, this precaution helps prevent two students working on the same data from sharing their results, thereby maintaining the effectiveness of double-keying for error prevention.

### 3.2 | Conversion of Original Measurements Units

The final verified digitised data files were converted to a pipe separated common data format designed by the C3S2-311 team for future processing. The common data format consists of 19 columns of identifier information, location information, temporal information, quality information and observation value information. The datetimes for observations in all stations were also converted from local time to Coordinated Universal Time (UTC). Some of the original observations required conversion to the WMO recommended International System of Units (SI).

Wind speed was originally recorded in three different units; Beaufort scale, kilometres per hour, meters per second and these varied throughout the record. The SI unit for wind is metres per second (m/s). The equation used to convert the Beaufort-scale wind speed observations to m/s is as follows:  $W = 0.836 \times B^{1.5}$ , where  $W$  is wind speed in m/s and  $B$  is value (integer from 0 to 12) on the Beaufort scale. This equation calculates the appropriate median values for that Beaufort-number and is approximated to the nearest integer. The equation used to convert the kilometres per hour wind observations to metres per second is as follows:  $1 \text{ (km/h)} = 1000/3600 \text{ (m/s)}$ . Given the inconsistencies

in wind speed measurement units throughout the historical record and the subjectivity of the Beaufort scale, caution is advised when interpreting the wind speed data. Wind direction was converted from Cardinal directions to degrees of the compass with 'Calm' entries in the 'Observed value' field left empty and 'Calm' text string entered in the measurement code field for reference. Caution in comparing these cardinal converted directions to modern wind direction measurements typically at c.1 degree resolution is advised.

The air pressure data was original recorded in millibars (mb) but required either adding 900 or 1000 mb depending on the station notes. All precipitation and temperature observations were originally recorded in SI units of millimetres (mm) and degrees Celsius (°C).

### 3.3 | Postprocessing of Data to Enable Analysis of Madagascar Stations

We analyse and present the results in later sections for three Madagascar stations with the longest records; Ambodifotatra (1955–1960), Andapa (1949–1960), and Nosy Varika (1951–1964). The complete data set for Andapa (1949–1960) was analysed combining the digitised records from this project and all previous projects. Moramanga and Morombe and the two CAR stations are omitted from the analysis, due to limited years of digitised records at this time.

To identify particularly hot periods, this paper calculates the monthly maximum temperatures for the selected stations in Madagascar derived from daily maximum temperature observations. The calculations apply the 3/5 rule, whereby any month containing more than three consecutive missing daily temperature records or more than 5 missing days in total is excluded from the computation. This quality control approach ensures the reliability and accuracy of the monthly temperature averages by minimising the impact of incomplete data (Anderson and Gough 2018). The analysis then highlights periods at the stations in Madagascar where monthly mean maximum temperatures exceeded the 90th percentile threshold for three or more consecutive months, indicating a particularly hot period.

The monthly accumulated precipitation is calculated from the daily values to identify extreme periods. The analysis excludes months where over 10% of daily precipitation records are missing, ensuring data reliability. The monthly precipitation records at Ambodifotatra, Andapa and Nosy Varika are then analysed using the Standardised Precipitation Index (SPI). SPI is a widely adopted and versatile drought index used to quantify precipitation anomalies over different timescales, such as monthly, seasonal or annual periods (Van Loon 2015; Lloyd-Hughes and Saunders 2002; Redmond 2002; Guttman 1999; McKee et al. 1993). By comparing the observed precipitation to averages over the period of record, the SPI provides a standardised measure of how wet or dry a particular period is relative to the climatological average (McKee et al. 1993). Positive SPI values indicate wetter than average conditions, while negative SPI values signify drier than average conditions (Jenkins and Warren 2015). The severity of these deviations is classified into categories ranging from mild to extreme, enabling detailed assessments of drought

and wetness intensity (Hayes et al. 2011; Guttman 1999). SPI values between 0.99 and  $-0.99$  are generally considered to be near normal, SPI values between  $\pm 1.00$  to  $\pm 1.49$  is classed as moderate,  $\pm 1.50$  to  $\pm 1.99$  is a severe period and  $\pm 2.00$  is an extreme period (WMO 2012). For this analysis, the SPI-3 (3-month accumulation periods) were calculated, which is commonly used to monitor seasonal crop moisture needs, assess short term water availability and is useful for identifying the onset of drought or wet conditions, making it a valuable tool for short-term planning and response (WMO 2012; McKee et al. 1993).

The station level pressure at Ambodifotatra, Andapa and Nosy Varika was also analysed to identify potential tropical cyclones over the period of record. The station level pressure data included observations taken daily at 7 AM, 12 PM and 5 PM local time, over the period 1949–1964. Typically, tropical cyclones are characterised by a sudden drop in pressure with significant low-pressure anomalies below an approximate sea level pressure of 1000 hPa (Emanuel 2005; Gray 1968; Petterssen 1956). The station level pressure threshold value of 1000 hPa was adjusted at each station based on the standard atmospheric lapse rate, accounting for the station elevation above sea level (asl) as described in Holton (2004). For low elevation stations, the pressure difference between sea level and a station at height can be approximated using a simple linear form of the hydrostatic equation, where,

- $\Delta P$  = pressure offset (in hPa),
- hhh = station elevation above sea level (in meters),
- $\rho$  = air density ( $\approx 0.225 \text{ kg/m}^3$  at sea level),
- g = gravitational acceleration ( $9.81 \text{ m/s}^2$ ),
- Division by 100 converts Pa to hPa (1 hPa = 100 Pa).

This linear approximation assumes standard atmospheric conditions, including a constant air density and temperature near sea level (Holton 2004). For example the Nosy Varika and Ambodifotatra stations, are both approximately 10 meters asl, the offset is estimated as:  $\Delta P = 0.12 \times 10 = 1.2 \text{ hPa}$ . Therefore, the adjusted station level pressure threshold was calculated as follows:  $P_{\text{threshold, station}} = 1000 - 1.2 \text{ hPa} = 998.8 \text{ hPa}$ . Likewise the Andapa station is at 470 m asl and therefore the threshold for identifying potential cyclone is adjusted to 943.6 hPa using the formula:  $\Delta P = 0.12 \times 470 = 56.4 \text{ hPa}$ .

### 3.4 | Documentary Sources

Documentary evidence is explored to validate the occurrence of, and assess the socio-economic impacts resulting from specific extreme events identified in the Madagascar data. Open access digital and searchable historical print media were accessed through the Irish Newspaper Archive (Irish Newspaper Archives, n.d.), and the Trove Australian newspaper archives (National Library of Australia, n.d.). Many of these newspapers began publishing in the early to mid-18th century, and some continue to operate to present day and have regularly reported global events. To identify news articles, yearly and monthly filters derived from specific data analysis results were used and combined key words such as ‘Madagascar’, ‘floods’, and

‘cyclone’ to reveal some interesting and informative articles. We also extract, translate and present information from two old French journal articles, that provide some interesting details and accounts of the impacts from the identified extreme events (Aldegheri 1959; Saboureaux 1959).

### 3.5 | Comparison Between Newly Digitised Data at Nosy Varika and ERA5 Hourly Data on Single Levels From 1940 to Present

To highlight the value of this newly digitised data we accessed the ERA-5 reanalysis data (Copernicus Climate Change Service, Climate Data Store 2023) to see how the rescued observations have the potential to improve dynamical reconstructions of impactful extreme events in this region. Using the coordinates of stations Nosy Varika and Ambodifotatra we were able to download the ERA-5 reanalysis hourly mean ensemble station pressure data for a particular month of interest from <https://cds.climate.copernicus.eu/datasets/reanalysis-era5-single-levels?tab=download>. We chose times of day for the ERA-5 data at 7.00 AM, 12 noon and 6.00 PM that matched the data observations times recorded at Nosy Varika and Ambodifotatra. First, the two datasets were plotted and the differences between corresponding values were calculated and also plotted. The mean bias was then computed to evaluate the average tendency of the reanalysis to over- or under-estimate the observed pressures. The root mean square error (RMSE) was calculated to quantify the magnitude of the errors, and the Pearson correlation coefficient was determined to assess the strength and consistency of the relationship between the observations and the reanalysis data.

## 4 | Results

### 4.1 | Initial Quality Control Results

The results of the mismatched value check on the data digitised in the 2024 project showed that most errors occurred due to issues with students keying the incorrect or inconsistent decimal places for the values, as shown in Figure 4. These were relatively simple to fix because it was usually a consistent error within 1 month of data. Other issues occurred, where a student had misread the value and clearly entered the wrong variable values into a column, this issue was also easily fixed by the checker. Figure 5 presents some actual misread incorrect keyed values for cloud observations (denoted as cld) and dry bulb temperature (denoted as dbt). Another identified error was the wrong year or month being entered on the template sheets, although not prevalent, this error did take a bit more time to investigate and fix.

Table 2 presents the keying error statistics for all five stations that were double keyed in the 2024 project. The results for Form Type 1 (precipitation and evaporation observations) indicate that Moramanga and Birao had the highest error rates, with more than 20% of observations affected at these stations. Stations Morombe, Bambari, and Nosy Varika exhibited fewer than 8% keying errors. There appears to be no obvious reason for the disparity in error rates across stations, as all data image sheets are uniformly formatted, of good quality, and all values are clearly visible.

File 'Form1\_Moramanga\_5\_1964.xlsx': Mismatch at Row 1, Column 2 (precip\_17) (Value1: 4.3, Value2: 43)  
 File 'Form1\_Moramanga\_5\_1964.xlsx': Mismatch at Row 1, Column 3 (precip7) (Value1: 0.8, Value2: 8)  
 File 'Form1\_Moramanga\_5\_1964.xlsx': Mismatch at Row 1, Column 4 (total\_precip) (Value1: 5.4, Value2: 52)  
 File 'Form1\_Moramanga\_5\_1964.xlsx': Mismatch at Row 1, Column 5 (evap\_18) (Value1: 0.7, Value2: 7)  
 File 'Form1\_Moramanga\_5\_1964.xlsx': Mismatch at Row 1, Column 6 (evap\_7) (Value1: 0.4, Value2: 1)  
 File 'Form1\_Moramanga\_5\_1964.xlsx': Mismatch at Row 1, Column 7 (evap\_total) (Value1: 0.8, Value2: 8)  
 File 'Form1\_Moramanga\_5\_1964.xlsx': Mismatch at Row 2, Column 5 (evap\_18) (Value1: 0.7, Value2: 7)  
 File 'Form1\_Moramanga\_5\_1964.xlsx': Mismatch at Row 2, Column 6 (evap\_7) (Value1: 0.4, Value2: 1)  
 File 'Form1\_Moramanga\_5\_1964.xlsx': Mismatch at Row 2, Column 7 (evap\_total) (Value1: 0.8, Value2: 8)  
 File 'Form1\_Moramanga\_5\_1964.xlsx': Mismatch at Row 3, Column 2 (precip\_17) (Value1: 1.9, Value2: 19)  
 File 'Form1\_Moramanga\_5\_1964.xlsx': Mismatch at Row 3, Column 3 (precip7) (Value1: 0.9, Value2: 9)  
 File 'Form1\_Moramanga\_5\_1964.xlsx': Mismatch at Row 3, Column 4 (total\_precip) (Value1: 2.8, Value2: 28)  
 File 'Form1\_Moramanga\_5\_1964.xlsx': Mismatch at Row 3, Column 5 (evap\_18) (Value1: 0.8, Value2: 8)  
 File 'Form1\_Moramanga\_5\_1964.xlsx': Mismatch at Row 3, Column 6 (evap\_7) (Value1: 0.2, Value2: 2)  
 File 'Form1\_Moramanga\_5\_1964.xlsx': Mismatch at Row 3, Column 7 (evap\_total) (Value1: 1.0, Value2: 10)  
 File 'Form1\_Moramanga\_5\_1964.xlsx': Mismatch at Row 4, Column 2 (precip\_17) (Value1: 3.3, Value2: 33)  
 File 'Form1\_Moramanga\_5\_1964.xlsx': Mismatch at Row 4, Column 3 (precip7) (Value1: 2, Value2: 20)  
 File 'Form1\_Moramanga\_5\_1964.xlsx': Mismatch at Row 4, Column 4 (total\_precip) (Value1: 5.3, Value2: 53)  
 File 'Form1\_Moramanga\_5\_1964.xlsx': Mismatch at Row 4, Column 5 (evap\_18) (Value1: 0.5, Value2: 5)  
 File 'Form1\_Moramanga\_5\_1964.xlsx': Mismatch at Row 4, Column 6 (evap\_7) (Value1: 0.4, Value2: 1)  
 File 'Form1\_Moramanga\_5\_1964.xlsx': Mismatch at Row 4, Column 7 (evap\_total) (Value1: 0.6, Value2: 6)  
 File 'Form1\_Moramanga\_5\_1964.xlsx': Mismatch at Row 5, Column 5 (evap\_18) (Value1: 1.2, Value2: 12)

FIGURE 4 | Snapshot of a mismatched value output file showing examples of some of the decimal place keying errors made by students.

File 'Form2\_Moramanga\_5\_1964.xlsx': Mismatch at Row 11, Column 19 (cld\_17) (Value1: 2, Value2: 4)  
 File 'Form2\_Moramanga\_5\_1964.xlsx': Mismatch at Row 12, Column 17 (cld\_7) (Value1: 7, Value2: 8)  
 File 'Form2\_Moramanga\_5\_1964.xlsx': Mismatch at Row 12, Column 19 (cld\_17) (Value1: 7, Value2: 2)  
 File 'Form2\_Moramanga\_5\_1964.xlsx': Mismatch at Row 13, Column 18 (cld\_12) (Value1: 1, Value2: 6)  
 File 'Form2\_Moramanga\_5\_1964.xlsx': Mismatch at Row 13, Column 19 (cld\_17) (Value1: 1, Value2: 2)  
 File 'Form2\_Moramanga\_5\_1964.xlsx': Mismatch at Row 14, Column 17 (cld\_7) (Value1: 3, Value2: 5)  
 File 'Form2\_Moramanga\_5\_1964.xlsx': Mismatch at Row 14, Column 18 (cld\_12) (Value1: 7, Value2: 6)  
 File 'Form2\_Moramanga\_5\_1964.xlsx': Mismatch at Row 14, Column 19 (cld\_17) (Value1: 3, Value2: 7)  
 File 'Form2\_Moramanga\_5\_1964.xlsx': Mismatch at Row 15, Column 18 (cld\_12) (Value1: 6, Value2: 4)  
 File 'Form2\_Moramanga\_5\_1964.xlsx': Mismatch at Row 15, Column 19 (cld\_17) (Value1: 4, Value2: 1)  
 File 'Form2\_Moramanga\_5\_1964.xlsx': Mismatch at Row 17, Column 9 (dbt\_12) (Value1: 197, Value2: 157)  
 File 'Form2\_Moramanga\_10\_1964.xlsx': Mismatch at Row 1, Column 2 (min\_t) (Value1: 11.9, Value2: 119)  
 File 'Form2\_Moramanga\_10\_1964.xlsx': Mismatch at Row 1, Column 3 (max\_t) (Value1: 25.8, Value2: 258)  
 File 'Form2\_Moramanga\_10\_1964.xlsx': Mismatch at Row 1, Column 5 (dbt\_7) (Value1: 17.6, Value2: 176)  
 File 'Form2\_Moramanga\_10\_1964.xlsx': Mismatch at Row 1, Column 6 (wbt\_7) (Value1: 15.1, Value2: 154)  
 File 'Form2\_Moramanga\_10\_1964.xlsx': Mismatch at Row 1, Column 9 (dbt\_12) (Value1: 24.8, Value2: 248)

FIGURE 5 | Snapshot of a mismatched value output file showing examples of some of the keying errors made by students where either rows or columns had been misassigned by one of the students yielding a mismatch.

The results for Form Type 2 (temperature, cloud and humidity observations) show that Bambari had the highest error rate at 17.4%, followed by Birao at 15.4% and Morombe at 12.6%. The results at the remaining two stations were much lower; Moramanga recorded an error rate of 9.8%, while Nosy Varika had 5.7%.

The results for Form Type 3 (pressure and wind observations) revealed that Morombe had the highest error rate at 23.1%. As before, some forms contained incorrect dates, but the main issue was mismatched wind direction letter case (e.g., Value1: wsw, vs.

Value2: WSW), which was easily corrected. Moramanga, Birao and Bambari recorded error rates of 10.9%, 11.8% and 10.7%, respectively, while Nosy Varika had an error rate below 5%.

The results indicate that Nosy Varika, the longest station, had the fewest keying errors, with error rates showing below 6% across all form types. Upon reviewing the data image sheets, the C3S2-311 team noted that, unlike the other stations, Nosy Varika's sheets featured clear and consistently formatted values without commas. This likely made it easier for students to read and enter the correct values with the proper decimal placement.



The C3S2-311 team observed that some returned forms contained incorrect date information, which caused mismatch errors in the data. The C3S2-311 team will reiterate the date entry requirements in future project instructions. However, most errors in Form Type 1 resulted from incorrect or inconsistent use of decimal places. This issue affected all stations except Nosy Varika. For example, precipitation and evaporation values are recorded in tenths of millimetres with leading zeros and, in some cases, include commas (e.g., 002 or 621). Similarly, some temperature and humidity values across different stations include commas while others do not (e.g., 2650 vs. 2825). These varying data formats appear to have confused some students when entering decimal values. The C3S2-311 team will ensure that guidance on decimal placement is clarified in future project instructions. Additionally, some wind observations in Form Type 3 were difficult to interpret. In particular, wind direction, recorded in cardinal directions, was often hard to read due to poor or smudged handwriting, contributing to keying errors. Many errors, however, were caused by mismatched letter case (e.g., Value1: wsw vs. Value2: WSW); the Python code has been updated to account for this issue going forward.

Through this rigorous quality control process, the team produced a fully verified set of digitised data files for each station based on the original images. This verification process took a C3S-team member 1-month to complete for the double keyed 2024 data, whereas the single keyed 2023 data files took around 3-months to complete the checks. Table 3 presents details of the

number of observations that were digitised for each station by each variable type. Over the two follow on CliDaR-Africa projects in 2023 and 2024 the students digitised over 315,000 observations for Madagascar and 71,000 observations for CAR.

## 4.2 | Initial Data Analysis Results

### 4.2.1 | Hot Periods

Figure 6 presents monthly maximum temperatures (°C) for Ambodifotatra, Andapa and Nosy Varika in Madagascar from 1949 to 1964 derived from daily temperature observations. Table 4 highlights periods at three stations in Madagascar where these monthly mean maximum temperatures (°C) exceeded the 90th percentile threshold for 3 or more consecutive months at each station.

The results at Ambodifotatra reveal two hot periods, the first occurred from January to March 1959, the second from December 1959 to February 1960, both lasting 3 months when monthly mean maximum temperatures reached or exceeded the 90th percentile (note this is austral summer period). Andapa results show that two extremely hot 3-month periods occurred between January 1954 and March 1954 and again between January 1955 to March 1955. Most notably the results for Nosy Varika show a 4-month severe hot period started in January 1961 persisting until April 1961.

**TABLE 2** | Presents the error statistics for stations digitised in 2024 (Morombe, Moramanga, Bambari, Birao and Nosy Varika) when double keying checks were conducted.

	Form type 1 keying errors	Total of values keyed	% of errors	Form type 2 keying errors	Total of values keyed	% of errors	Form type 3 keying errors	Total of values keyed	% of errors
Morombe	4954	340	6.9%	9906	1250	12.6%	7471	1729	23.1%
Moramanga	6003	1224	20.4%	8948	879	9.8%	7387	874	11.8%
Bambari	8387	494	5.9%	15,760	2744	17.4%	10,821	1161	10.7%
Birao	7203	1506	20.9%	14,265	2197	15.4%	7185	789	10.9%
Nosy Varika	15,302	799	5.2%	45,142	2581	5.7%	45,237	2114	4.7%

Note: Form 1 Type = precipitation and evaporation observations, Form Type 2 = temperature, cloud and humidity observations and Form Type 3 = pressure and wind observations.

**TABLE 3** | The number of observations by variable for each station that have been digitised by students over the two projects in 2023 and 2024.

	Ambodifotatra	Nosy Varika	Andapa	Morombe	Moramanga	Bambari	Birao
Temperature	18,681	45,142	10,650	7400	6590	10,506	10,704
Precipitation	6025	15,302	4990	2465	2648	4199	3656
Pressure	6524	15,130	4320	2551	2500	2818	0
Wind	11,819	30,107	8640	4920	4887	8003	7185
Water vapour/humidity	3245	0	4990	2489	2456	9353	7180
Cloud	6214	15,093	273	2506	2358	3940	3561
Total observations	52,508	120,774	33,863	22,331	21,439	38,819	32,286

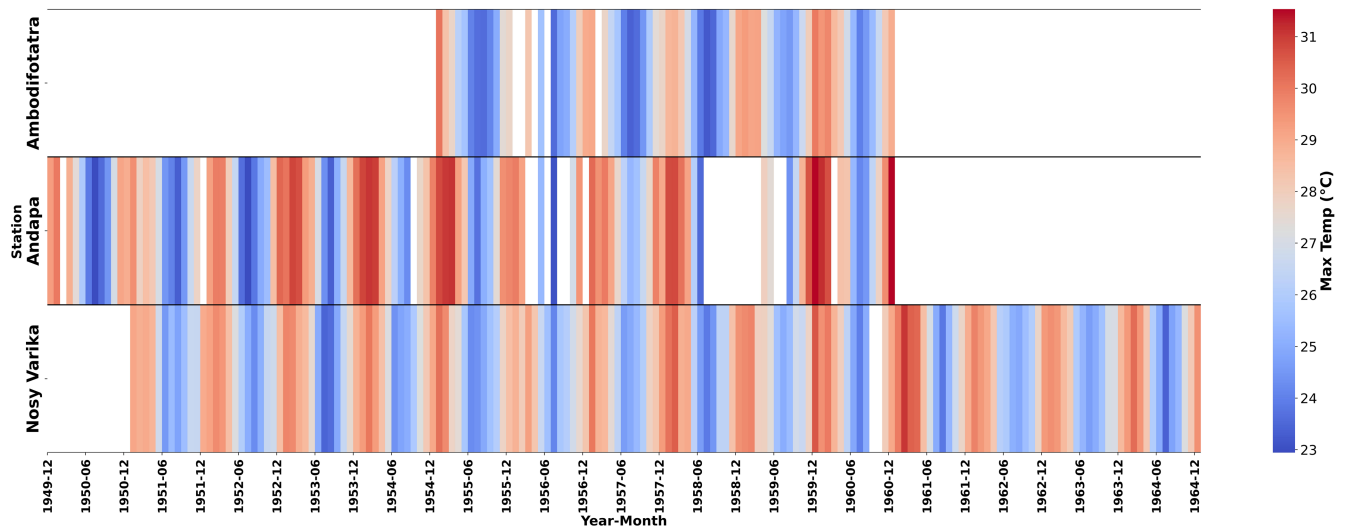


**FIGURE 6** | Monthly maximum mean temperatures (°C) for the three stations in Madagascar from 1949 to 1964, calculated from daily values using the 3/5 rule. Colours range from blue indicating colder conditions to red for hotter conditions and are presented in the style of Ed Hawkins warming stripes (<https://showyourstripes.info/>). Any month with more than three consecutive missing daily values or more than five missing daily values in total was excluded from the calculation. [Colour figure can be viewed at [wileyonlinelibrary.com](https://onlinelibrary.wiley.com)]

**TABLE 4** | Identified hot periods at each station, where the monthly mean maximum temperature (°C) exceeded the 90th percentile threshold for 3 or more consecutive months.

Station	Year-month	Monthly mean maximum temperature (°C)	90th Percentile (°C)
Ambodifotatra	1959–01	29.3	29.1
Ambodifotatra	1959–02	29.1	29.1
Ambodifotatra	1959–03	29.2	29.1
Ambodifotatra	1959–12	30.0	29.1
Ambodifotatra	1960–01	29.5	29.1
Ambodifotatra	1960–02	29.7	29.1
Andapa	1954–01	30.9	30.6
Andapa	1954–02	31.1	30.6
Andapa	1954–03	31.0	30.6
Andapa	1955–01	30.8	30.6
Andapa	1955–02	31.0	30.6
Andapa	1955–03	31.1	30.6
Nosy Varika	1961–01	30.0	29.7
Nosy Varika	1961–02	31.1	29.7
Nosy Varika	1961–03	30.5	29.7
Nosy Varika	1961–04	30.4	29.7

*Note:* The table includes the station name, start and end dates of each hot period, and the corresponding monthly mean temperatures during these periods and corresponding 90th percentile temperature.

4.2.2 | Precipitation Extremes

Figure 7 presents the SPI-3 analysis results from the monthly accumulated precipitation. Table 5 results show that Ambodifotatra experienced a severe 2-month drought: November 1960 to December 1960, with the maximum SPI-3 intensity value reaching (−1.92). A further 1-month drought occurred in October

1959, and had a maximum SPI-3 intensity value of (−1.84). Andapa experienced one severe drought event during November 1950 (SPI-3 = −1.61).

The analysis for Nosy Varika identifies several drought events over the 14 years of available data. The most notable 3-month drought event occurred from September 1956 to November

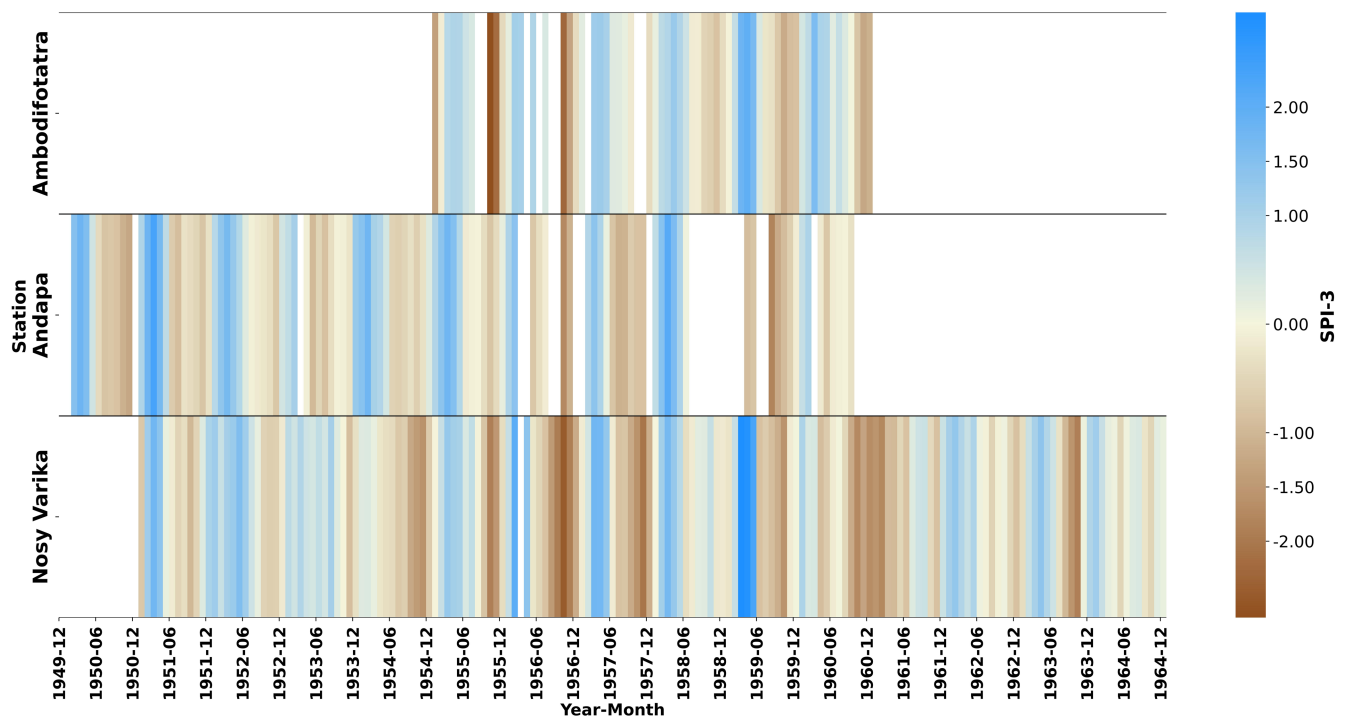


**FIGURE 7** | Plot of calculated SPI-3 values from the monthly summed precipitation (mm) with data months with over 10% missing days filtered out for selected stations in Madagascar from 1949 to 1964. The heatmap represents extreme drought to extreme wetness, with colours ranging from brown (dry conditions, negative SPI values, range from  $-2.5$ ) to blue (wet conditions, positive SPI values, values range to  $+2.9$ ), zero indicates normal conditions. [Colour figure can be viewed at [wileyonlinelibrary.com](https://onlinelibrary.wiley.com/doi/10.1002/joc.70203)]

1956 reaching a maximum SPI-3 value of ( $-2.50$ ), indicative of exceptional drought conditions. The second most noteworthy 3-month drought event was experienced in December 1960 to February 1961, reaching a maximum SPI-3 intensity value of ( $-1.75$ ). There were two further 2-month drought events at Nosy Varika. The first occurred between October 1957 and November 1957 and showed a maximum SPI-3 intensity value of ( $-2.05$ ), the second event was September 1963 to October 1963 and recorded a maximum SPI-3 intensity value of ( $-1.89$ ). There were another four single month duration drought events at Nosy Varika with SPI-3 values ranging from ( $-1.56$  to  $-1.88$ ).

These results underscore the intensity and recurrence of severe drought episodes at Nosy Varika during the period 1951–1964. Under the Köppen–Geiger climate classification (Peel et al. 2007), Nosy Varika has a classic tropical rainforest climate (Af), characterised by warm, humid, and very wet conditions, with an increased risk of tropical cyclones during the summer months. Although September and October are Nosy Varika's driest months, the region usually experiences consistent precipitation throughout the year, making the identified droughts particularly remarkable. Moreover, many of these droughts appeared to have emerged during or near the monsoon season (November to April), a period when Madagascar usually receives most of its annual precipitation. Droughts during this period can have critical knock-on effects and can lead to severe water shortages, crop failures, livestock stress, and heightened food insecurity (Rigden et al. 2024).

Table 6 provides results from the SPI-3 analysis, focusing on periods where the SPI-3 value exceed the threshold of ( $+1.5$ ).

According to McKee et al. (1993) instances exceeding this threshold are indicative of significantly above-average precipitation over a three-month period, which can have considerable hydrological, infrastructural and ecological implications.

The results presented in Table 6 indicate that Ambodifotatra's most notable extreme long duration precipitation period occurred in early 1959, from March to May reaching a maximum SPI-3 intensity of ( $+2.2$ ), indicating extreme wet conditions. A further one-month severe precipitation period occurred during March 1960 with a maximum SPI-3 intensity of ( $+1.7$ ). For Andapa, the analysis identified three 2-month duration precipitation periods. The first occurred between March and April 1950, with a maximum SPI-3 intensity of ( $+1.8$ ). The most extreme 2-month duration precipitation period occurring during March to April 1951 and recorded a maximum SPI-3 intensity of ( $+2.4$ ). The third 2-month precipitation period occurred between March and April 1958 and had a maximum SPI-3 intensity of ( $+2.2$ ). The remaining precipitation periods at Andapa were 1-month duration periods and have SPI-3 values ranging from ( $+1.6$  to  $+1.7$ ).

Nosy Varika experienced several severe precipitation periods between 1951 and 1964. The most notable, as identified in the Ambodifotatra's results, occurred over a 3-month period starting in March 1959, with a maximum SPI-3 intensity reaching ( $+2.9$ ), continuing through April (SPI-3 =  $+2.8$ ), and then into May (SPI-3 =  $+2.3$ ). These results uncover an exceptionally intense precipitation period during March 1959. Nosy Varika received 1452 mm of total rainfall, a 615% increase above the normal monthly March precipitation of 203 mm (calculated over the 1991–2020 period) for Madagascar (World Bank 2025b).



**TABLE 5** | The summary of outcomes of the SPI-3 analysis, specifically highlighting all instances where SPI-3 values fall below (−1.5).

Station	Year and month	SPI-3 value
Ambodifotatra	1959–10	−1.84
Ambodifotatra	1960–11	−1.92
Ambodifotatra	1960–12	−1.73
Andapa	1950–11	−1.61
Nosy Varika	1954–11	−1.60
Nosy Varika	1955–10	−1.88
Nosy Varika	1956–09	−1.94
Nosy Varika	1956–10	−2.50
Nosy Varika	1956–11	−1.91
Nosy Varika	1957–10	−1.59
Nosy Varika	1957–11	−2.05
Nosy Varika	1959–10	−1.56
Nosy Varika	1960–10	−1.72
Nosy Varika	1960–12	−1.68
Nosy Varika	1961–01	−1.54
Nosy Varika	1961–02	−1.75
Nosy Varika	1963–09	−1.54
Nosy Varika	1963–10	−1.89

Note: This threshold signifies the onset of severe drought conditions, as per the SPI classification system (McKee et al. 1993; WMO 2012).

Remarkably, nearly double the normal March monthly precipitation (385 mm) fell in just 1 day on March 29, 1959 at Nosy Varika. Another notable extreme precipitation period occurred at Nosy Varika in February 1956, with a maximum SPI-3 intensity value of (+2.1). Additionally, a 2-month extreme period was recorded at Nosy Varika during March 1957 to April 1957, and reached a maximum SPI-3 intensity of (+1.8). A further four 1-month precipitation periods were identified during; March 1951, May 1952, February 1956 and March 1958, with SPI-3 values ranging from (+1.6 to +2.1).

#### 4.2.3 | Tropical Cyclones

The first potential cyclone event at Ambodifotatra (Figure 8, top-plot) occurred when the pressure dropped from 1000.5 hPa at 12 noon down to 995.4 hPa at 5 PM on 25 January 1956. The pressure the following morning at 7 AM on the 26 January fell to 995.0 hPa. According to NOAA (n.d.), the Historical Hurricane Tracks tool shows that there was an unnamed tropical depression which began on the 19 January 1956 in the Indian Ocean just off the north-east coast of Madagascar. On the 21 January it developed into a category 1 cyclone with maximum wind speeds of 65 knots (120 km/h), making landfall directly over Ambodifotatra on the 25 January between 6 PM and 12 midnight. As it passed over Madagascar from north east to west it

**TABLE 6** | The results of the SPI-3 analysis and all values that exceed an SPI-3 of +1.5 which indicated a severe wet period.

Station	Year and month	SPI-3
Ambodifotatra	1959–03	2.0
Ambodifotatra	1959–04	2.2
Ambodifotatra	1959–05	1.7
Ambodifotatra	1960–03	1.7
Andapa	1950–03	1.8
Andapa	1950–04	1.5
Andapa	1951–03	2.4
Andapa	1951–04	1.7
Andapa	1952–03	1.6
Andapa	1954–02	1.7
Andapa	1955–03	1.7
Andapa	1958–03	2.2
Andapa	1958–04	1.6
Nosy Varika	1951–03	1.8
Nosy Varika	1952–05	1.6
Nosy Varika	1956–02	2.1
Nosy Varika	1957–03	1.8
Nosy Varika	1957–04	1.7
Nosy Varika	1958–03	1.7
Nosy Varika	1959–03	2.9
Nosy Varika	1959–04	2.8
Nosy Varika	1959–05	2.3

weakened to a tropical storm with reduced wind speeds of 35 knots (65 km/h). The wind data at Ambodifotatra recorded wind speeds of 6.7 m/s (24 km/h) at 7 AM, 9.4 m/s (33.8 km/h) at 12 noon, and 15.5 m/s (55.8 km/h) at 5 PM on the 25 January 1956. On the 26 January the Ambodifotatra records show wind speeds of 22.6 m/s (81.4 km/h) at 7 AM, 9.4 m/s (33.8 km/h) at 12 noon and then the wind speed reduces to 2.4 m/s (8.6 km/h) at 5 PM as the storm moves away.

The second potential tropical cyclone was identified on the 25 March 1959. The pressure at Ambodifotatra dropped from 1001.4 hPa at 12 noon down to 996 hPa at 5 PM on the 25 March, rising to 1000 hPa at 7 AM. This corresponds with an unnamed category 1 cyclone that developed as a tropical depression off the north east coast of Madagascar at 6 AM on the 22 March 1959 (NOAA n.d.). The cyclone moved towards the northern region of Madagascar and made landfall just north of Ambodifotatra on the 25 March at 6 PM with maximum wind speeds of 65 knots (120 km/h). The wind data at Ambodifotatra showed that wind speeds peaked at 16.9 m/s (60.8 km/h) at 5 PM on the 25 March 1959 dropping down to 4.2 m/s (15.1 km/h) at 7 AM on the 27 March as the cyclone moved away.

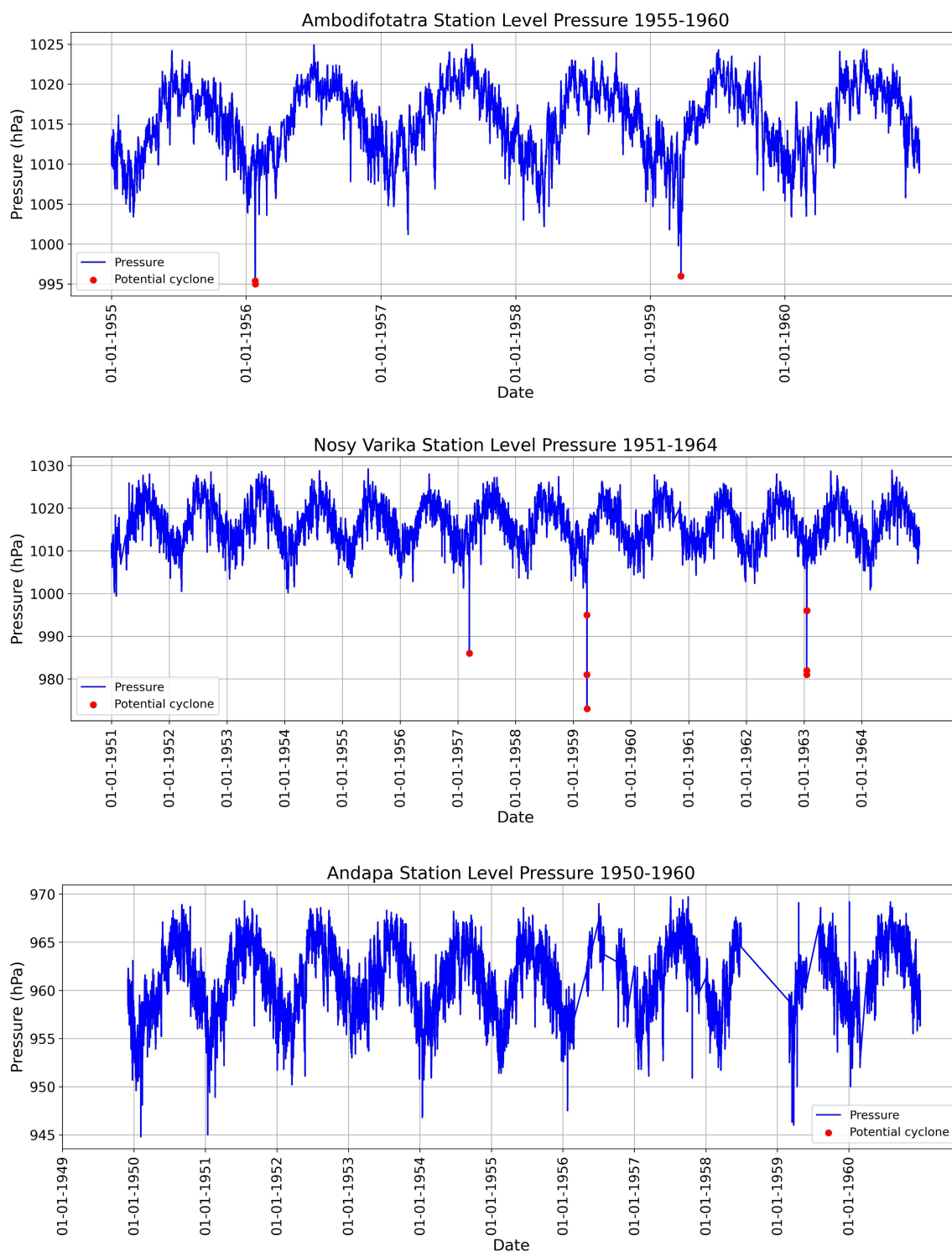


**FIGURE 8** | Potential tropical cyclone events at the three stations in Madagascar. Blue traces denote normal pressure values with red dots highlighting pressure values below the allocated threshold to identify a potential cyclone for each station based on the station altitude. Thresholds applied are: Ambodifotatra 10m asl (998.8 hPa), Andapa 470m asl (943.6 hPa), and Nosy Varika 10m asl (998.8 hPa) (see Section 2 for further details). [Colour figure can be viewed at [wileyonlinelibrary.com](https://onlinelibrary.wiley.com/doi/10.1002/joc.70203)]

The results of the station level pressure analysis at Nosy Varika (Figure 8 middle-plot) identified three potential tropical cyclone events over the period 1951–1964. The first occurred on 14 March 1957 when the pressure drops from 1003.3 hPa at 7 AM, to 1000.9 hPa at 12 noon and then reduces to 986.0 hPa at 5 PM. Unfortunately, there is no documented evidence of a

tropical cyclone or tropical storm hitting Nosy Varika or eastern Madagascar on the 14 March 1957. In addition, the wind speed data at Nosy Varika do not show any major increases around this date. The precipitation data did not reveal any particularly extreme events on the 14 March 1957, but it was a particularly wet period from March to April 1957. The original value was

checked and deemed to be entered correctly as per the original data sheet, so this may have been a temporary instrument measurement issue or potential observer keying error. If future quality checks deem these values to be suspicious they will be flagged.

The second potential cyclone is identified on the 28 into the 29 March 1959 and shows a drop in pressure from 1000.6 hPa at 5 PM local time on 28 March down to 973.0 hPa by 7.00 AM on the 29 March. The Nosy Varika wind data also shows that wind speeds peaked at 9.4 m/s (33.8 km/h) at 7 AM and 12 noon on the 28 March and again at 7 AM on the 29 March. These results correspond with the results presented for Ambodifotatra and relate to the same cyclone identified around this date. The Historical Hurricane Tracks tool shows that on the 26 into 27 March the now tropical depression moved inland and south-westward, but swung left towards the east coast again, impacting Nosy Varika on the 28 March (NOAA n.d.). Section 4.3 will provide more in-depth details on this particular extreme cyclonic event.

The third potential cyclone identified at Nosy Varika occurred on 17 January 1963. The results show that pressure dropped from 1004.8 hPa at 5 PM on the 16 January to 981.0 hPa at 12 noon on the 17 January. The results also show that although pressure increased slightly to 1001.0 hPa at 7 AM on the 18 January it dropped again to 996.0 hPa at 12 noon and 5 PM on the same day. The Nosy Varika wind data shows that wind speeds of 6.7 m/s (24.1 km/h) were recorded throughout the 17 and 18 January and peaked at 22.6 m/s (81.4 km/h) at 5 PM on the 18 January. This relates to cyclone Delia that developed on the 9 January 1963 several hundreds of kilometres off the east coast of Madagascar (NOAA n.d.). Fortunately, this powerful cyclone, with maximum wind speeds of 75 knots (140 km/h), did not make landfall on Madagascar (NOAA n.d.). However, Delia moved close to the mid-eastern coastline of Madagascar on 17 and 18 January 1963 causing some impacts on the coastal settlements including Nosy Varika. The precipitation data at Nosy Varika show that 19.5 mm fell on the 15 January, another 58.7 mm was observed on the 16 January and a further 19.5 mm recorded on the 17 January 1963.

The results at Andapa (Figure 8, bottom-plot) show that the threshold of 943.6 hPa for identifying potential tropical cyclones was not breached. However, the results do show some low pressure values close to the threshold. These occurred on the 5 February 1950 (944.8 hPa), 13 January 1951 (945.0 hPa), 25 March 1959 (946.0 hPa), 17 March 1959 (946.3 hPa), 13 January 1954 (946.8 hPa) and the 26 March 1959 (946.9 hPa). The results for March 1959 at Andapa are consistent with the cyclone identified at Ambodifotatra and Nosy Varika around these dates. Unfortunately, the March 1959 precipitation records for Andapa are missing from the series.

### 4.3 | Documentary Evidence of Extreme Weather Events Across Madagascar During March 1959

The initial data analysis revealed several noteworthy extreme events. Here we focus on the March 1959 unnamed cyclones that particularly impacted Nosy Varika and Ambodifotatra both located on the east coast of Madagascar.

An online search revealed that only two articles reported on the March 1959 cyclones. Both articles are in French but the translated text states that two intense cyclones impacted the east coast and high plateaus of Madagascar during March 1959 (Aldegheri 1959; Saboureau 1959). The first cyclone formed as a low-pressure system on 14 March 1959, as the depression headed towards southern Madagascar it strengthened and intensified. By 16 March heavy rain was falling along the north-eastern coast from the Masoala Peninsula to Mananjary moving westward at c.18 km/h. The system deepened and became a category 1 cyclone and making landfall on 17 March around 1.00 PM UTC. The eastern region experienced sustained wind speeds over 100 km/h with torrential rainfall (Aldegheri 1959; Saboureau 1959).

In Tamatave, which was located more than 300 km away from the centre of the cyclone 'During the night of March 16 to 17, their intensity is such that a port crane, weighing more than 100 tons, is pushed over 100 meters, while the SS Caplane, at anchor, drags on its anchor and nearly gets thrown ashore' (Aldegheri 1959). The article also noted that at the weather station of Île Sainte-Marie; 'The precipitation is heavy: 49.9 mm on the 16th; 128.4 mm on the 17th; 229 mm on March 18th' (Aldegheri 1959). The cyclone continued to slowly move across northeastern plateaus of Madagascar and as it travels across land it weakened in strength, but still 'causes very abundant precipitation over all the eastern regions' (Aldegheri 1959). On the 20 March the cyclone moved out to sea and gains intensity once more, with heavy rain persisting along the east coast. By 22 March, the depression had shifted eastward, while a strengthening anticyclonic system settled south of the region. The disturbance near Mananjary, still fed by equatorial and trade winds, slowed and stalled about 120 miles offshore. On 23 March, conditions had changed significantly as a new cyclone formed in northeast of Saint-Brandon disrupting the equatorial inflow, causing the cyclone over Mananjary to weaken. Luckily, the core of the first cyclone did not make landfall in any major urban areas, and with wind gusts only ranging from 95 to 100 km/h only limited damage was reported, but extremely heavy rainfall was experienced along the eastern coast causing severe flooding. Figure 9 presents images taken from Aldegheri (1959) and shows the impacts in the aftermath of the 1959 cyclones in Madagascar.

Figure 10 shows the trajectory of the first cyclone and provides some highlights of the rainfall amounts, wind speeds and minimum pressure values recorded across major towns on Madagascar's east coast during March 1959. The most notable rainfall amounts were recorded at Mahanoro which received 637.4 mm between the 16 and 21 March (Aldegheri 1959). Tamatave, received 602.5 mm of rainfall in just 4 days from 16 to 19 March. Wind speeds in Tamatave were estimated to have peaked at 27.8 m/s (100 km/h) on 16 and 17 March. Wind speeds in Ambodifotatra, on the island of Île Sainte-Marie, reached 28 m/s (98.4 km/h) between 18 and 20 March and the air pressure dropped to 999.3 hPa.

On 22 March, a swift eastward movement of a mobile polar trough occurred, causing a high-pressure system to intensify south of Madagascar and the Mascarene Islands. While a small-diameter cyclone remained off Madagascar's southeast coast,



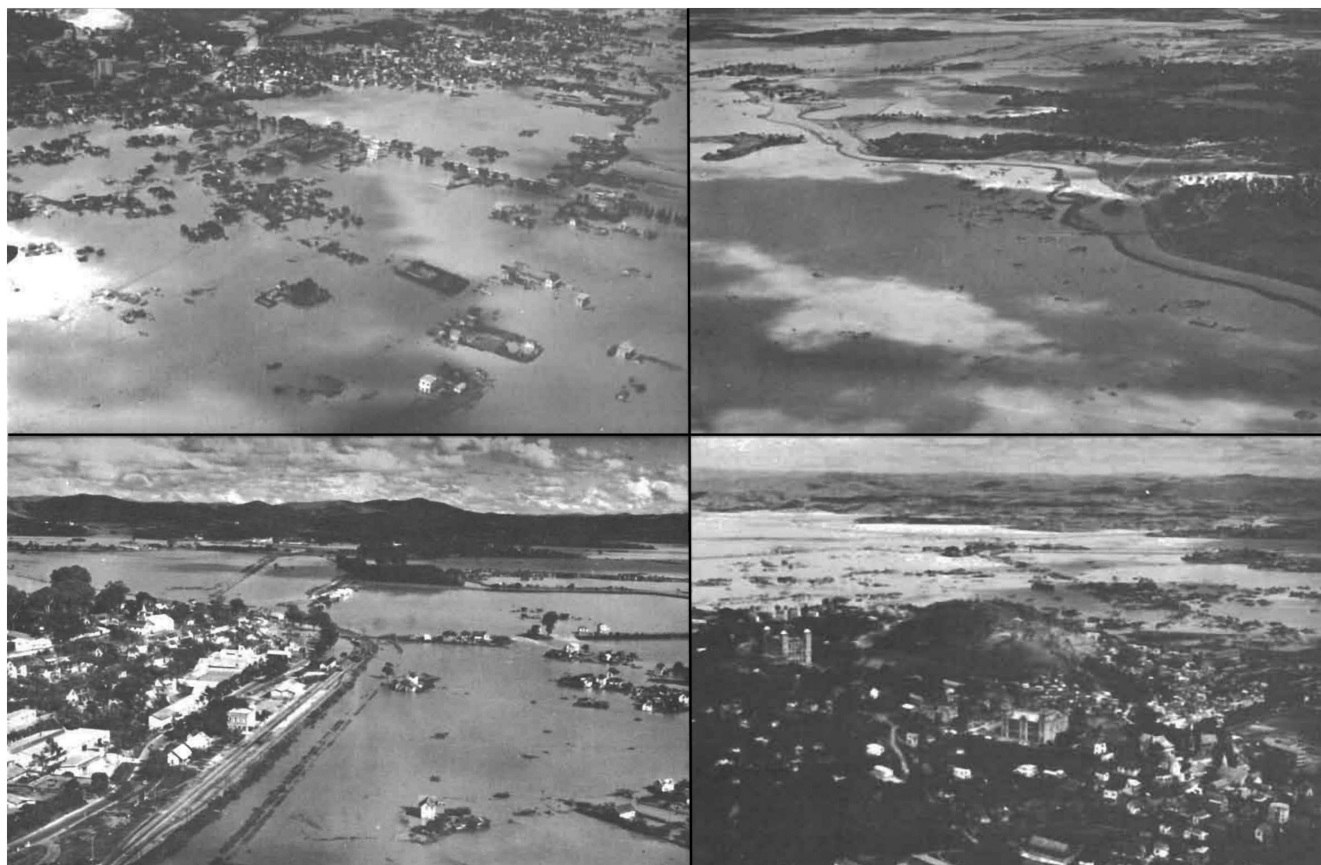


**FIGURE 9** | Images showing the impacts after the March 1959 cyclones that hit Madagascar. Top left image is the harbour quarter in the capital Tananarive, the top right shows Tananarive's Lake Mandrozeza, bottom left image is the rural town of Sonierana, in the Analanjirofo Region and bottom right shows the Anosizato zone in Tananarive. Images taken from (Aldegheri 1959).

the overall atmospheric pressure continued to rise. Easterly winds strengthened south of the Intertropical Convergence Zone (ITCZ) and at higher altitudes, a cyclonic curvature persisted. However, a pilot's weather report from Mahé in the Seychelles noted a shift in the equatorial current, changing direction from west-northwest on 21 March to west-southwest by 06:00 UTC on the 22. The loss of north-westerly inflow, caused the southern cyclone to weaken. In contrast, one of the disturbances within the ITCZ rapidly intensified on the night of the 22 March, developing into a moderate, then strong tropical depression (Aldegheri 1959). During the 23 March this tropical depression continued to deepen and evolved into the second cyclone during the night.

On 24 March, the second cyclone continued to intensify as it moved west-southwest at 10 knots (18.52 km/h) towards Tromelin Island. A rapid pressure drop was noted at 07:00 UTC, with sustained wind speeds reaching 148 km/h by 15:00 UTC, gusting to over 51 m/s (185 km/h), causing damage to the Tromelin Island weather station anemometer. At 18:00 UTC a minimum pressure of 949.6 hPa was recorded at Tromelin Island as the cyclone's centre passed just north of the island the winds speeds were greater than 55.6 m/s (200 km/h). No calm centre eye-feature was observed and the cyclone continued on a west-southwest track towards Madagascar. In Tamatave, severe wind gusts were observed along the coast but again the anemometer failed to record the speed, probably due to damage from the wind gusts.

During the night of 25 March into the 26 the second March cyclone reached Madagascar's northeastern slopes over the northern highlands, just south of Mandritsara. By the afternoon on the 26 the cyclone had moved inland weakened and slowed down. Overnight the cyclone shifted southward in direction, slowing to 5 knots (9.26 km/h), now a broad cyclone that caused widespread heavy rain. On the 28 March, the cyclone passed near Maevatanana, moved through the Antananarivo region before coming close to Marolambo. Overnight on 28 March into the 29, the cyclone re-entered the ocean near Nosy Varika, causing rapid intensification again. The article mentions that from the night of the 28 March until the 29 March, 'the depression moves off the land at the height of Nosy-Varika and exceptionally heavy rainfall is recorded'. Travelling at around 10 knots, the cyclone neared Réunion Island but on 30 March it slowed and appeared to stall 60–80 nautical miles southwest of the island before gradually turning south-southwest. By 31 March, it started to move away from Réunion on a south-southwest trajectory. This cyclone was among the most violent ever recorded in the southwest Indian Ocean.

Figure 11 not only presents details of the trajectory of the second cyclone but also highlights rainfall amounts as well as wind speeds and some minimum pressure values from 23 March to 3 April 1959. The towns of Anivorano-Est, Mahanoro and Mananjary, along the eastern coast near Nosy Varika, received rainfall exceeding 600 mm between 24 and 29 March (Aldegheri 1959). In addition, wind speeds in Mahanara reached

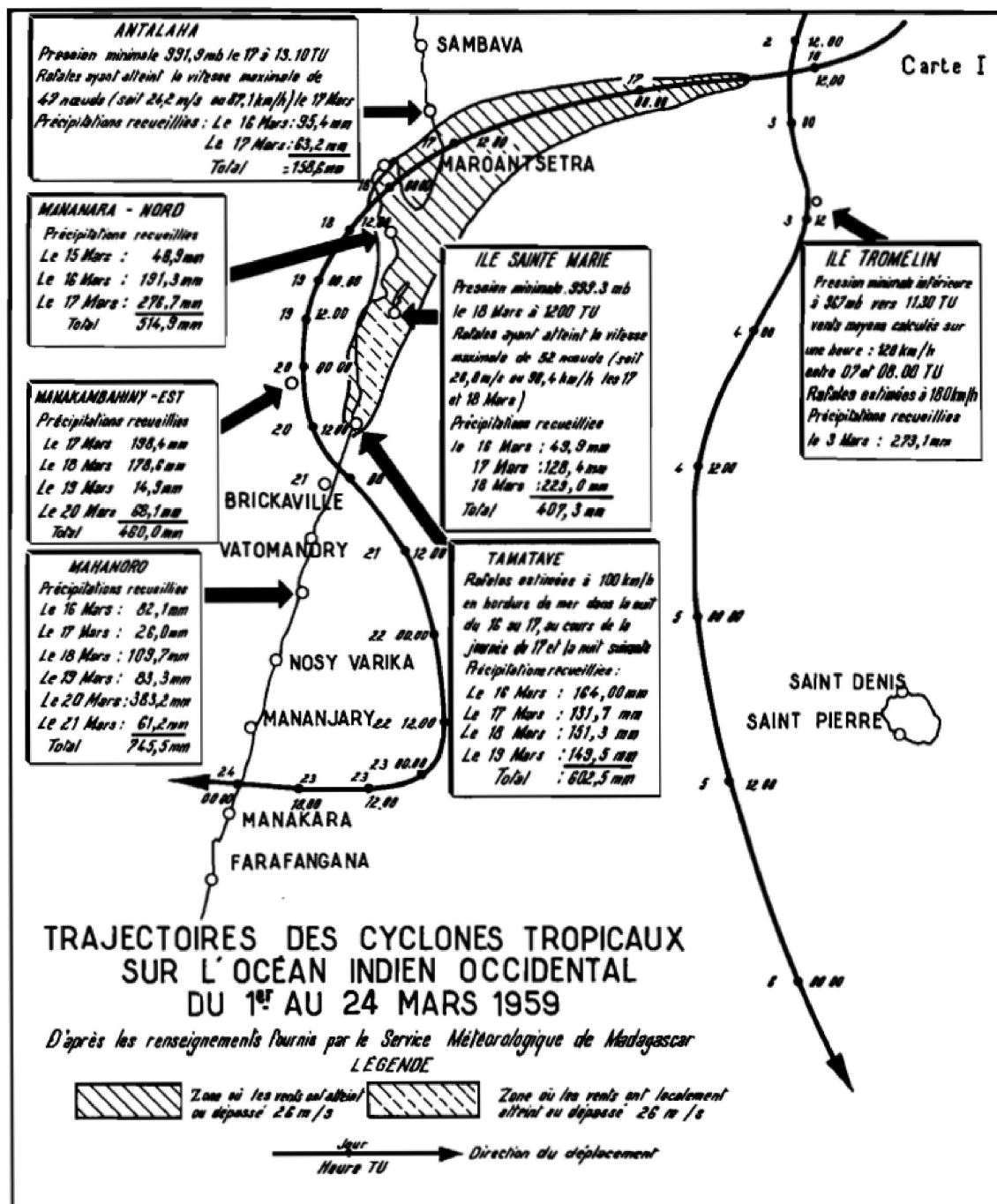


**FIGURE 10** | Summary of the trajectory of the first cyclone during March 1959 and providing some details of the amount of rainfall that fell across larger towns located on the east coast of Madagascar between 1 March and the 24 March 1959. The image also shows areas of extreme wind speeds denoted by \\\ on the map and provides some minimum pressure values. Image taken from Aldegheri (1959).

55 m/s (200 km/h) and a minimum pressure of 967 hPa was recorded. Ambodifotatra, located on the island of Île Sainte-Marie, saw wind speeds reach 40 m/s (144 km/h) and pressure drop to 992.8 hPa on 25 March.

Figures 10 and 11 show that both this cyclone and the previous one had similar trajectories and made landfall in nearly the same area of Madagascar. This meant that within only a few days the eastern coastal region between Mananara-Nord and Mananjary, including the Highlands was exposed twice to the severe impacts associated with tropical cyclones.

An online search of open access English language newspaper archives also revealed some documentary evidence that describes the violent storms that occurred during March 1959 in Madagascar. A newspaper article found in the National Library of Australia online archives (National Library of Australia, n.d.) from the Canberra Times published on the 31 March 1959 (page1) stated that 'Winds of 210 m.p.h., tropical rains and river floods have made more than 100,000 people homeless in Madagascar' it also noted that 'Forty thousand people were evacuated on Saturday night from Tananarive' and 'Whole plantations and villages have been swept away and damage runs into



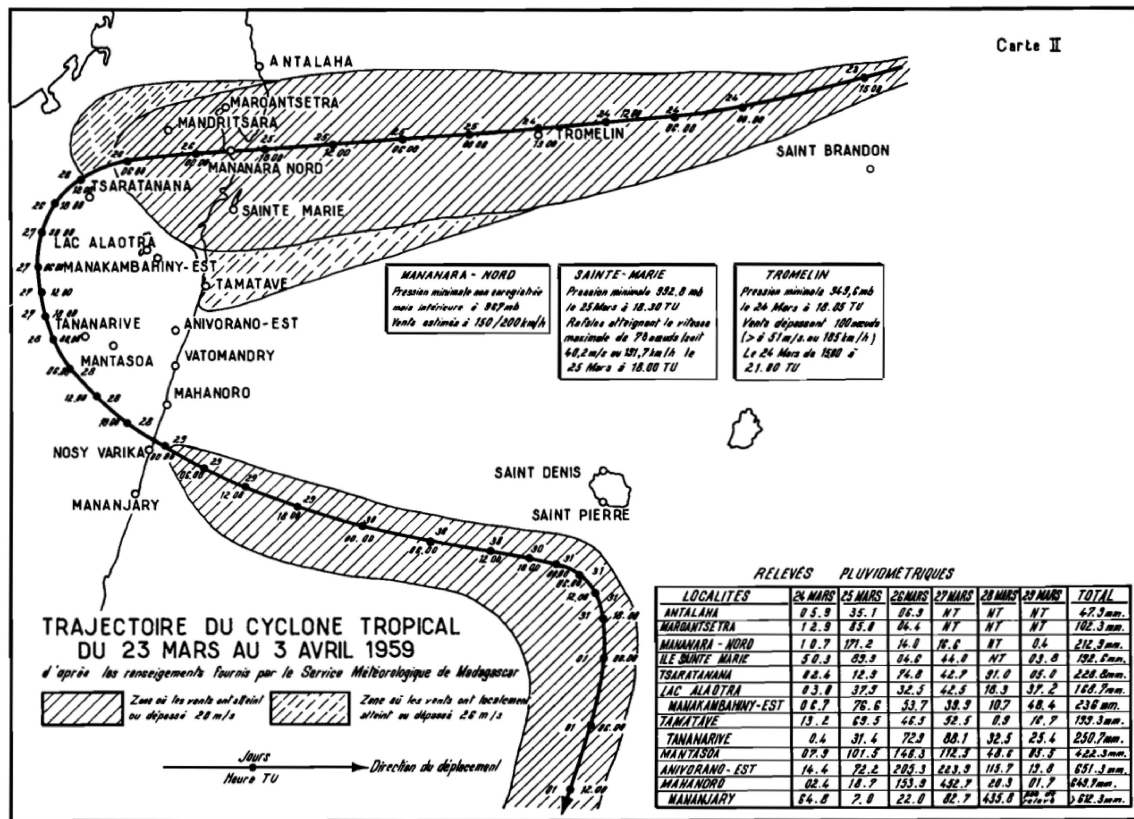


**FIGURE 11** | Illustration of the trajectory of the second cyclone during March 1959 providing some details of the amount of rainfall that fell across larger towns located on the east coast of Madagascar between 24 March and the 29 March 1959. The image also shows areas of extreme wind speeds denoted by \\\ on the map and provides some minimum pressure values for four main towns. Image taken from Aldegheri (1959).

millions of francs'. The Canberra Times on the 1 April (page 1) stated that although the French Air Force planes had dropped food supplies 'many isolated areas were reported to be down to their last supplies' and also noted that the capital Tananarive was completely covered in flood water that was continuing to rise (see Figure 12).

On the 2 April 1959 (page 6), the Canberra Times initially reported that over 3000 people were feared dead and over 200,000 people from Tananarive had been evacuated to higher ground (see Figure 12). The article goes on to say that a lack of communications has made it impossible to fully assess the number of casualties from remote areas. The article also states that there 'is a great danger of epidemics' due to polluted water.

Searchable historical print media were also accessed through the Irish Newspapers online archive (Irish Newspaper Archives n.d.) which provides over 300 years of newspaper articles. Many of these newspapers revealed some interesting articles on the Madagascar March 1959 cyclone's (see Figure 12). The Belfast Newsletter published on 27 March 1959, (page 5) initially reported that 20 people had died after a cyclone had hit the north-east coast of Madagascar the night before causing 'disastrous damage'. The Belfast Newsletter published on 4 April 1959 (page 3) and the Irish Examiner published on 4 April 1959 (page 9) both mention how 40,000 people were made homeless in the city of Tananarive and reported that some other towns

across Madagascar were so badly damaged that they will have to be completely rebuilt. The same articles also state that some regions were under six and half feet of mud with up to 40% of crops of rice, coffee and sugar destroyed. It was also noted that the French army were dropping emergency supplies to affected remote areas, but they were running out of parachutes (see Figure 12). Moreover, in the months immediately following the two cyclones, the region experienced additional extreme rainfall events (Table 5), likely compounding their impacts. There is also some interesting historical black and white film footage online from the British Pathé global newsreel archive, showing of the aftermath of these devastating cyclones during March 1959 in Madagascar (British Pathé 1959).

#### 4.4 | Results of Comparison Between Nosy Varika Pressure Observations and ECMWF ERA-5 Pressure Data

In this section, we present the results of the comparison between the newly digitised observation at Nosy Varika and Ambodifotatra and ECMWF ERA-5 reanalysis data. The analysis focuses on March 1959, when two cyclone events affected the eastern coast of Madagascar.

The first cyclone, which occurred between 18 and 20 March 1959, remained offshore of Nosy Varika. While it produced substantial rainfall, the winds had minimal impact on Nosy Varika.





**FIGURE 12** | Online newspaper articles showing reports on the extreme weather events during March 1959 in Madagascar. From top left to right; the Canberra Times Thursday 2 April 1959 (page 6), Irish Examiner published on 4 April 1959 (page 9), The Belfast Newsletter published on 14 April 1959 (page 8). From bottom left to right; the Canberra Times Wednesday 1 April 1959 (page 1), Belfast Newsletter published on 27 March 1959 (page 5), and the Canberra Times Thursday 31 March 1959 (page 1).

As a result, the observed surface pressures at Nosy Varika show no major effect from this system, and ERA-5 similarly reflects no significant pressure changes (Figure 13). The second cyclone passed directly over Nosy Varika on the 29 March 1959. The second cyclone producing a minimum pressure observation of 973.0 hPa at 07:00 UTC on the 29 March at Nosy Varika. As shown in Figure 13, ERA-5 underestimated the intensity of this event, producing a minimum pressure of 980.8 hPa on the 27 March at 12:00 UTC, and misrepresented the timing by nearly 2 days. These results provide direct evidence of the cyclone's intensity and timing at Nosy Varika, aspects that are only partially captured by the ERA-5 reanalysis.

The overall statistics for the comparison between Nosy Varika and ERA-5 data show a mean bias of +1.21 hPa indicating only a small systematic overestimation by ERA-5 relative to the station data (Figure 14). This bias is not atypical and results from the use of grid cell representative topographic values in ERA5. The results on the analysis between the datasets showed an RMSE of 5.89 hPa which suggests moderate random errors. The correlation coefficient of 0.42 shows that ERA-5 only partially reproduces the temporal variability observed at Nosy Varika.

The first cyclone passed over Ambodifotatra between 18 and 20 March and produced a modest drop in pressure, with

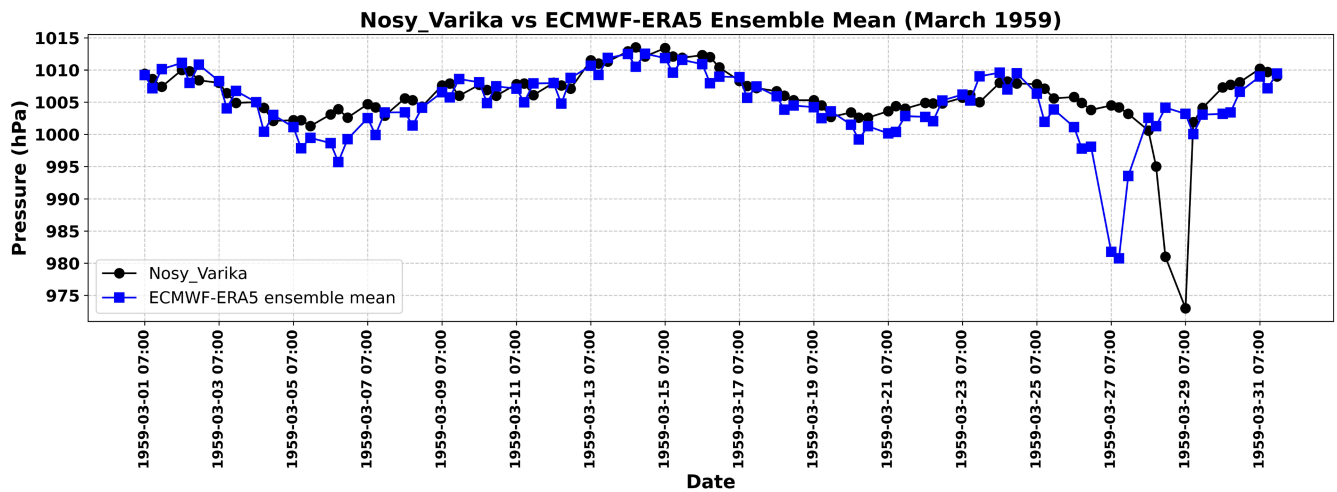


**FIGURE 13** | Timeseries plot showing Nosi Varika station pressure observations and ECMWF ERA-5 reanalysis ensemble mean station pressure data. [Colour figure can be viewed at [wileyonlinelibrary.com](https://onlinelibrary.wiley.com)]

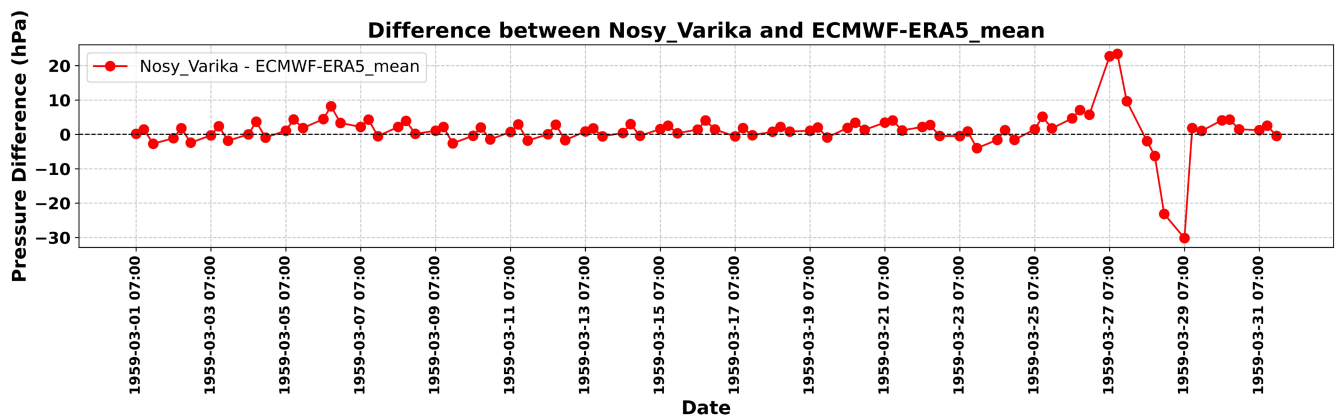


**FIGURE 14** | Difference between Nosi Varika station pressure observations and ECMWF ERA-5 reanalysis ensemble mean station pressure data. [Colour figure can be viewed at [wileyonlinelibrary.com](https://onlinelibrary.wiley.com)]

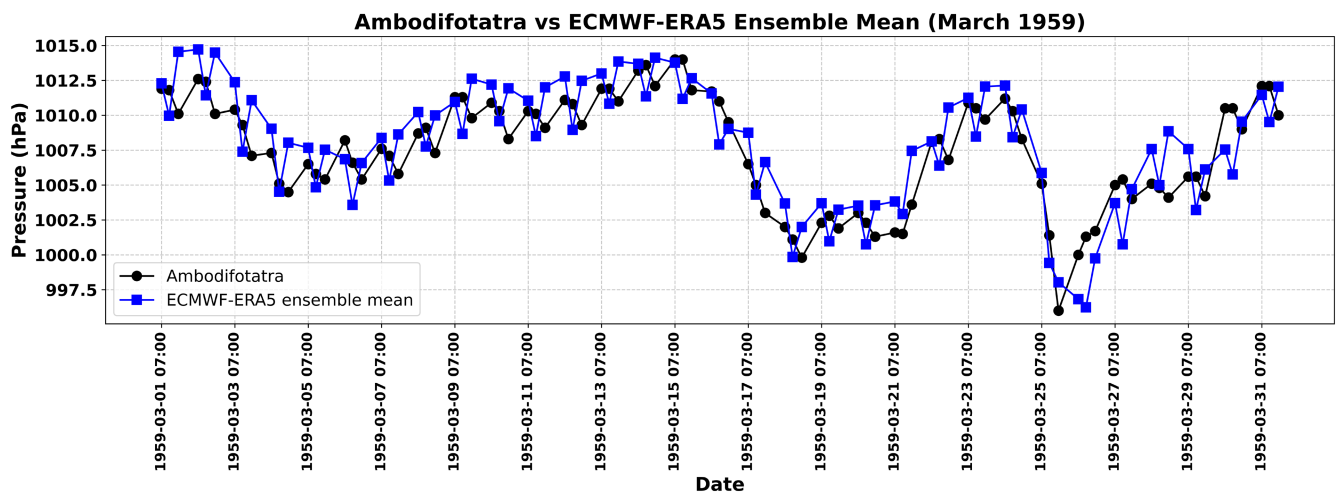


**FIGURE 15** | Timeseries plot showing Ambodifotatra station pressure observations and ECMWF ERA-5 reanalysis ensemble mean station pressure data. [Colour figure can be viewed at [wileyonlinelibrary.com](https://onlinelibrary.wiley.com)]

observations ranging from 1003.0 down to 999.8 hPa. ERA-5 captured the general trend of this low-pressure system, though small differences in magnitude and timing occurred (Figure 15).

The second cyclone hit Ambodifotatra on the 25 March, producing a station minimum of 996.0 hPa at 18:00 UTC, closely matched by ERA-5 at 996.2 hPa on 26 March 12:00 UTC,

indicating very good agreement in magnitude with a timing offset of 18 h clearly defined in Figure 15.

The difference between the Ambodifotatra observed values and the ERA-5 data are presented in Figure 16. The comparison between Ambodifotatra surface pressure observations and the ERA-5 reanalysis shows excellent overall agreement during March 1959. The mean bias of  $-0.37$  hPa indicates only a slight overestimation by ERA-5, while the RMSE of 2.28 hPa reflects small random errors. The correlation coefficient of 0.85 demonstrates a strong match in temporal variability.

In summary, ERA-5 reproduces general surface pressure patterns and minor events reasonably well at both stations. However, the comparison with the newly digitised surface pressure observations at Nosy Varika highlights notable discrepancies during the passage of the cyclone on the 29 March 1959, particularly in the magnitude and timing of the extreme low-pressure event. At Ambodifotatra, minor differences and timing offsets exist between ERA-5 and the observations during March 1959. Nevertheless, the reanalysis captures both the general pressure variability and the cyclone-induced pressure drops with some accuracy. These results underscore the critical value of the newly digitised observations. By incorporating this digitised data into ECMWF reanalysis datasets, the representation of extreme events, local pressure minima, and temporal variability can be improved. Moreover, this will lead to more accurate reanalysis reconstructions for the region. Such good quality historical observations are essential for refining reanalysis products, validating model performance, and enhancing our understanding of past extreme events.

## 5 | Future Work and Data Availability and Concluding Remarks

### 5.1 | Future Work

Since inception back in 2022, the MU CliDaR-Africa students have digitised over 64 years of unique data in Madagascar, Guinea and Central African Republic. This equates to nearly 450,000 meteorological observations. This new data enhances

coverage in these data-sparse regions, supporting more robust climate extremes assessments and future climate projections crucial for adaptation planning. Student feedback has been very positive, highlighting skill development and a sense of contributing to a meaningful real-world project (Noone et al. 2024). The C3S2-311 team plans to use all feedback to improve the project's educational impact in future iterations. The CliDaR-Africa project will continue to run in the second year Geography skills module at students at MU, initially focussing on completing the unique data at Madagascar to produce some long continuous records from the 1940's to date.

The project has only begun to address the challenge of digitising the millions of images in the ACMAD collection. To further this effort, personal networks and academic peers are continually being contacted at other universities and institutes, encouraging them to adopt the CliDaR-Africa data rescue model and inspire similar student-driven projects. For example, a recent opportunity to engage visiting students from the University of Kentucky enabled digitisation of additional records and they are now considering the potential to integrate into their formal curriculum (Healion et al. 2025). The C3S2-311 team has also been exploring ways to adapt the CliDaR-Africa project to enable secondary school students across Ireland to participate in digitising key African meteorological records.

The initial data analysis presented in this paper highlights the importance and utility of this data and shows the value of documentary evidence to confirm the extremes contained therein. The results highlight the significant vulnerability of Madagascar to extreme weather events such as hot periods, droughts and heavy precipitation, and in particular tropical cyclones. The information presented in Section 4 highlights the importance of understanding the patterns and impacts of these weather extremes to inform mitigation and adaptation strategies. The findings also present valuable insights into some of the socio-economic impacts of these frequent natural hazards in the region. Furthermore, once fully digitised and integrated with contemporary records the historical data for Madagascar will allow for a more comprehensive reconstruction of past climate. In turn, enabling the assessment of changes over time, and provide a basis for predicting future climate-related challenges.

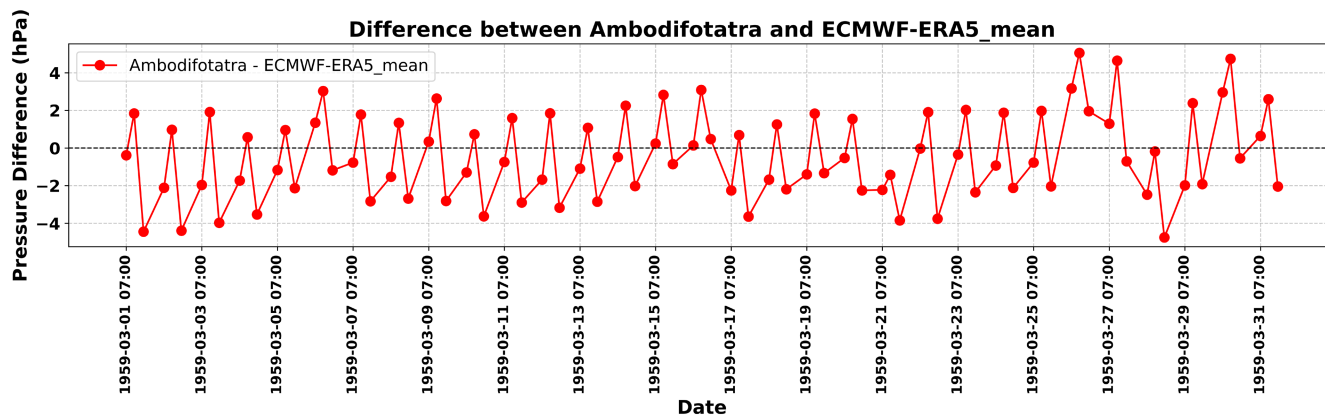


**FIGURE 16** | Difference between Ambodifotatra station pressure observations and ECMWF ERA-5 reanalysis ensemble mean station pressure data. [Colour figure can be viewed at [wileyonlinelibrary.com](https://onlinelibrary.wiley.com)]



Moreover, the ingestion of these newly digitised data into global reanalysis data products will lead to more accurate outputs for this region.

## 5.2 | Data Availability

The digitised data for this paper in a common data format is accessible from Pangaea data repository (<https://doi.org/10.1594/PANGAEA.983618>). All the data image sheets and completed original data template forms are stored in the C3S2-311 servers and are available on request. The digitised data will also be merged or appended to any existing data and quality controlled using state of the art methods (Dunn et al. 2022; Dunn et al. 2014; Dunn et al. 2012; Menne et al. 2012; Durre et al. 2010) and then integrated into the next data release of the C3S2-311 Collection and Processing of In Situ Observations database. The data will be made openly and freely available to data users in a common format via the Copernicus Climate Data Store (Copernicus Climate Change Service 2021) and the National Oceanic and Atmospheric Administration's (NOAA) National Centers for Environmental Information (NCEI) data centre in the US (National Centers for Environmental Information, n.d.). The newly digitised data will also be assimilated in ECMWF reanalysis data products, such as the soon to be released ERA-6 reanalysis (ECMWF 2024).

## 6 | Concluding Remarks

Projects such as the CliDaR-Africa project allow students to contribute to real world research, gain new useful skills and deepen their understanding of climate change. Such projects also help students gain experience in working with complicated data and allow them to problem solve potential issues, while boosting climate literacy and engagement. Ultimately, students can take pride in knowing they have contributed to progressing global climate science and contributed to increasing the climate data coverage in a particularly data sparse region such as Africa.

Finally, if your university or institute is interested in participating in the CliDaR-Africa data rescue project, please reach out to the corresponding author. We can provide access to images, templates, and other materials to support your engagement.

### Author Contributions

**Simon Noone:** conceptualization, investigation, writing – original draft, methodology, validation, visualization, writing – review and editing, software, formal analysis, data curation. **Caoilfhionn D'Arcy:** writing – review and editing, conceptualization, data curation. **Kevin Healion:** conceptualization, writing – review and editing, validation, data curation. **Peter Thorne:** conceptualization, writing – review and editing, funding acquisition, project administration.

### Acknowledgements

The authors would like to thank Copernicus/ECMWF for funding the rescuing of this invaluable data into digital images from the degrading microfiche film. In addition, this project could not have been completed without the help of the MU second year Geography undergraduate student cohorts during 2022, 2023 and 2024 in digitising this data.

### Funding

The Service is funded by Copernicus C3S under contract 2021/C3S2\_311\_Lot1\_NUIM led by Maynooth University, Ireland.

### Conflicts of Interest

The authors declare no conflicts of interest.

### Data Availability Statement

The data that support the findings of this study are openly available in Pangaea at <https://doi.pangaea.de/10.1594/PANGAEA.983618>.

### References

- Aldegheri, M. 1959. "Cyclones of March 1959 in Madagascar." In *Hydrological Yearbook of Overseas France: Year 1957*, 33–55. ORSTOM. [https://horizon.documentation.ird.fr/exl-doc/pleins\\_textes/divers12-05/16864.pdf](https://horizon.documentation.ird.fr/exl-doc/pleins_textes/divers12-05/16864.pdf).
- Allan, R., P. Brohan, G. P. Compo, R. Stone, J. Luterbacher, and S. Brönnimann. 2011. "The International Atmospheric Circulation Reconstructions Over the Earth (ACRE) Initiative." *Bulletin of the American Meteorological Society* 92: 1421–1425. <https://doi.org/10.1175/2011BAMS3218.1>.
- Anderson, C. I., and W. A. Gough. 2018. "Accounting for Missing Data in Monthly Temperature Series: Testing Rule-Of-Thumb Omission of Months With Missing Values." *International Journal of Climatology* 38: 4990–5002. <https://doi.org/10.1002/joc.5801>.
- Ashcroft, L., J. R. Coll, A. Gilabert, et al. 2018. "Rescued Dataset of Sub-Daily Meteorological Observations for Europe and the Southern Mediterranean Region, 1877–2012." *Earth System Science Data* 10, no. 3: 1613–1635. <https://doi.org/10.5194/essd-10-1613-2018>.
- British Pathé. 1959. "Madagascar Floods [film]. Archive, British Pathé." <https://www.britishpathe.com/asset/196051/>.
- Brönnimann, S. 2022. "Historical Observations for Improving Reanalyses." *Frontiers in Climate* 4: 880473. <https://doi.org/10.3389/fclim.2022.880473>.
- Brönnimann, S., R. Allan, L. Ashcroft, et al. 2019. "Unlocking Pre-1850 Instrumental Meteorological Records a Global Inventory." *Bulletin of the American Meteorological Society* 100, no. 12: ES389–ES413. <https://doi.org/10.1175/BAMS-D-19-0040.1>.
- Brönnimann, S., Y. Brugnara, R. J. Allan, et al. 2018. "A Roadmap to Climate Data Rescue Services." *Geoscience Data Journal* 5, no. 1: 28–39. <https://doi.org/10.1002/gdj3.56>.
- Brunet, M., and P. Jones. 2011. "Data Rescue Initiatives: Bringing Historical Climate Data Into the 21st Century." *Climate Research* 47: 29–40. <https://doi.org/10.3354/cr00960>.
- Brunet, M., P. D. Jones, S. Jourdain, D. Efthymiadis, M. Kerrouche, and C. Boroneant. 2013. "Data Sources for Rescuing the Rich Heritage of Mediterranean Historical Surface Climate Data." *Geoscience Data Journal* 1: 61–73. <https://doi.org/10.1002/gdj3.4>.
- Chimani, B., I. Auer, M. Prohom, M. Nadbath, A. Paul, and D. Rasol. 2022. "Data Rescue in Selected Countries in Connection With the EUMETNET DARE Activity." *Geoscience Data Journal* 9, no. 1: 187–200. <https://doi.org/10.1002/gdj3.128>.
- Churchill, W. n.d. "The Farther Backward You Can Look, The Farther Forward You Are Likely To See." <https://winstonchurchill.org/resources/quotes/>.
- Copernicus Climate Change Service (C3S). 2021. "Global Land Surface Atmospheric Variables From 1755 to 2020 From Comprehensive In-Situ Observations (Version 1)." <https://cds.climate.copernicus.eu/cdsapp#!/dataset/insitu-observations-surface-land?tab=overview>.

- Copernicus Climate Change Service (C3S). 2024. "Historical In-Situ Observations are Essential For Copernicus' Flagship Reanalysis Dataset." Copernicus In-Situ. <https://insitu.copernicus.eu/resources/use-cases-folder/historical-in-situ-observations-are-essential-for-copernicus-flagship-reanalysis-dataset>.
- Copernicus Climate Change Service, Climate Data Store. 2023. "ERA5 Hourly Data on Single Levels From 1940 to Present. Copernicus Climate Change Service (C3S) Climate Data Store (CDS)." <https://doi.org/10.24381/cds.adbb2d47>.
- Craig, P. M., and E. Hawkins. 2024. "Digitizing Observations From the 1861–1875 Met Office Daily Weather Reports Using Citizen Scientist Volunteers." *Geoscience Data Journal* 11: 608–622. <https://doi.org/10.1002/gdj3.236>.
- Cram, T. A., G. P. Compo, X. Yin, et al. 2015. "The International Surface Pressure Databank Version 2." *Geoscience Data Journal* 2: 31–46. <https://doi.org/10.1002/gdj3.25>.
- Dinku, T. 2019. "Challenges With Availability and Quality of Climate Data in Africa." In *Extreme Hydrology and Climate Variability*, 71–80. Elsevier. <https://doi.org/10.1016/B978-0-12-815998-9.00007-5>.
- Dooley, K., C. Kelly, N. Seifert, et al. 2023. "Reassessing Long-Standing Meteorological Records: An Example Using the National Hottest Day in Ireland." *Climate of the Past* 19: 1–22. <https://doi.org/10.5194/cp-19-1-2023>.
- Dunn, R. J., C. Azorin-Molina, M. J. Menne, Z. Zeng, N. W. Casey, and C. Shen. 2022. "Reduction in Reversal of Global Stilling Arising From Correction to Encoding of Calm Periods." *Environmental Research Communications* 4, no. 6: 061003.
- Dunn, R. J., K. M. Willett, P. W. Thorne, et al. 2012. "HadISD: A Quality-Controlled Global Synoptic Report Database for Selected Variables at Long-Term Stations From 1973–2011." *Climate of the Past* 8, no. 5: 1649–1679.
- Dunn, R. J. H., K. M. Willett, C. P. Morice, and D. E. Parker. 2014. "Pairwise Homogeneity Assessment of HadISD." *Climate of the Past* 10, no. 4: 1501–1522.
- Durre, I., M. J. Menne, B. E. Gleason, T. G. Houston, and R. S. Vose. 2010. "Comprehensive Automated Quality Assurance of Daily Surface Observations." *Journal of Applied Meteorology and Climatology* 49: 1615–1633. <https://doi.org/10.1175/2010JAMC2375>.
- Emanuel, K. A. 2005. *Divine Wind: The History and Science of Hurricanes*. Oxford University Press.
- Engström, J. E., L. Wern, S. Hellström, et al. 2023. "C. Data Rescue of Historical Wind Observations in Sweden Since the 1920s." *Earth System Science Data Discussions* 15: 2259–2277. <https://doi.org/10.5194/essd-15-2259-2023>.
- Goodman, S. M., J. P. Benstead, and W. L. Jungers, eds. 2003. *The Natural History of Madagascar*. University of Chicago Press.
- Gray, W. M. 1968. "Global View of the Origin of Tropical Disturbances and Storms." *Monthly Weather Review* 96, no. 10: 669–700. [https://doi.org/10.1175/1520-0493\(1968\)096%3C0669:GVOTOO%3E2.0.CO;2](https://doi.org/10.1175/1520-0493(1968)096%3C0669:GVOTOO%3E2.0.CO;2).
- Guttman, N. B. 1999. "Accepting the Standardized Precipitation Index: A Calculation Algorithm." *Journal of the American Water Resources Association* 35, no. 2: 311–322. <https://doi.org/10.1111/j.1752-1688.1999.tb03592.x>.
- Hannah, L., D. Radhika, S. J. Andelman, and G. Midgley. 2008. "Climate Change, Tropical Forests, and Biodiversity." *Conservation Biology* 22, no. 1: 1–9. <https://doi.org/10.1111/j.1523-1739.2007.00852.x>.
- Harvey, C. A., Z. L. Rakotobe, N. S. Rao, et al. 2014. "Extreme Vulnerability of Smallholder Farmers to Agricultural Risks and Climate Change in Madagascar." *Philosophical Transactions of the Royal Society, B: Biological Sciences* 369, no. 1639: 20130089. <https://doi.org/10.1098/rstb.2013.0089>.
- Hawkins, E., P. Brohan, S. N. Burgess, et al. 2023. "Rescuing Historical Weather Observations Improves Quantification of Severe Windstorm Risks." *Natural Hazards and Earth System Sciences* 23: 1465–1482. <https://doi.org/10.5194/nhess-23-1465-2023>.
- Hawkins, E., S. Burt, P. Brohan, et al. 2019. "Hourly Weather Observations From the Scottish Highlands (1883–1904) Rescued by Volunteer Citizen Scientists." *Geoscience Data Journal* 6, no. 2: 160–173. <https://doi.org/10.1002/gdj3.79>.
- Hawkins, E., S. Burt, M. McCarthy, et al. 2023. "Millions of Historical Monthly Rainfall Observations Taken in the UK and Ireland Rescued by Citizen Scientists." *Geoscience Data Journal* 10, no. 2: 246–261. <https://doi.org/10.1002/gdj3.157>.
- Hayes, M. J., M. D. Svoboda, N. A. Wall, and M. Widhalm. 2011. "The Lincoln Declaration on Drought Indices: Universal Meteorological Drought Index Recommended." *Bulletin of the American Meteorological Society* 92, no. 4: 485–488. <https://doi.org/10.1175/2010BAMS3103.1>.
- Healion, K., C. D'Arcy, and S. Noone. 2025. "Collaborative Climate Data Rescue Workshop with visiting University of Kentucky Students. ICARUS Climate Research Unit (blog), 9 July." <https://icar-us-maynooth.blogspot.com/2025/07/collaborative-climate-data-rescue.html>.
- Hersbach, H. 2023. "ERA5 Reanalysis Now Available From 1940." Newsletter no. 175, European Centre for Medium-Range Weather Forecasts (ECMWF). <https://www.ecmwf.int/en/newsletter/175/news/era5-reanalysis-now-available-1940>.
- Holton, J. R. 2004. *An Introduction to Dynamic Meteorology*. 4th ed. Academic Press.
- Irish Newspaper Archives. n.d. "Irish Newspaper Archives." Accessed July 22, 2025. <https://www.irishnewsarchive.com>.
- Jenkins, K., and R. Warren. 2015. "Quantifying the Impact of Climate Change on Drought Regimes Using the Standardised Precipitation Index." *Theoretical and Applied Climatology* 120, no. 1–2: 41–54. <https://doi.org/10.1007/s00704-014-1143-x>.
- Kaspar, F., A. Andersson, M. Ziese, and R. Hollmann. 2022. "Contributions to the Improvement of Climate Data Availability and Quality for Sub-Saharan Africa." *Frontiers in Climate* 3: 815043. <https://doi.org/10.3389/fclim.2021.815043>.
- Kaspar, F., B. Tinz, H. Mächel, and L. Gates. 2015. "Data Rescue of National and International Meteorological Observations at Deutscher Wetterdienst." *Advances in Science and Research* 12: 57–61. <https://doi.org/10.5194/asr-12-57-2015>.
- Khan, M. J. U., F. Durand, M. Afroosa, et al. 2025. "Tropical Cyclone Induced Compound Flooding in Madagascar: A Coupled Modeling Approach." *Natural Hazards* 121: 11013–11050. <https://doi.org/10.1007/s11069-025-07209-z>.
- Lakkis, S. G., P. O. Canziani, J. O. Rodriguez, and A. E. Yuchechen. 2023. "Early Meteorological Records From Corrientes and Bahía Blanca, Argentina: Initial ACRE-Argentina Data Rescue and Related Activities." *Geoscience Data Journal* 10, no. 3: 328–346. <https://doi.org/10.1002/gdj3.176>.
- Liu, H. Y., M. Satoh, J. F. Gu, et al. 2023. "Predictability of the Most Long-Lived Tropical Cyclone Freddy (2023) During Its Westward Journey Through the Southern Tropical Indian Ocean." *Geophysical Research Letters* 50, no. 20: e2023GL105729.
- Lloyd-Hughes, B., and M. A. Saunders. 2002. "A Drought Climatology for Europe." *International Journal of Climatology* 22: 1571–1592. <https://doi.org/10.1002/joc.846>.
- Luterbacher, J., R. Allan, C. Wilkinson, et al. 2024. "The Importance and Scientific Value of Long Weather and Climate Records; Examples of

- Historical Marine Data Efforts Across the Globe.” *Climate* 12, no. 3: 39. <https://doi.org/10.3390/cli12030039>.
- McKee, T. B., N. J. Doesken, and J. Kleist. 1993. “The Relationship of Drought Frequency and Duration to Time Scales.” In *Proceedings of 8th Conference on Applied Climatology*, Vol. 17, No. 22, January, 179–183. <https://doi.org/10.1002/joc.337>.
- Menne, M. J., I. Durre, R. S. Vose, B. E. Gleason, and T. G. Houston. 2012. “An Overview of the Global Historical Climatology Network-Daily Database.” *Journal of Atmospheric and Oceanic Technology* 29: 897–910. <https://doi.org/10.1175/JTECH-D-11-00103>.
- Murphy, C., A. Coen, I. Clancy, et al. 2023. “The Emergence of a Climate Change Signal in Long-Term Irish Meteorological Observations.” *Weather and Climate Extremes* 42: 100608. <https://doi.org/10.1016/j.wace.2023.100608>.
- Nash, D. J., K. Pribyl, J. Klein, G. H. Endfield, D. R. Kniveton, and G. C. Adamson. 2015. “Tropical Cyclone Activity Over Madagascar During the Late Nineteenth Century.” *International Journal of Climatology* 35, no. 11: 2943–2958. <https://doi.org/10.1002/joc.4204>.
- National Centers for Environmental Information (NCEI). n.d. “National Centers for Environmental Information.” National Oceanic and Atmospheric Administration. Accessed July 22, 2025. <https://www.ncei.noaa.gov/>.
- National Hurricane Center. 2019. “The Saffir-Simpson Hurricane Wind Scale.” National Oceanic and Atmospheric Administration. Accessed July 14, 2025. <https://www.nhc.noaa.gov/aboutsshws.php>.
- National Library of Australia (NLA). n.d. “Trove.” Accessed July 22, 2025. <https://trove.nla.gov.au/>.
- National Oceanic and Atmospheric Administration (NOAA). n.d. “Historical Hurricane Tracks” Accessed July 29, 2025. <https://coast.noaa.gov/hurricanes/>.
- Noone, S., C. Atkinson, D. I. Berry, et al. 2021. “Progress Towards a Holistic Land and Marine Surface Meteorological Database and a Call for Additional Contributions.” *Geoscience Data Journal* 8: 103–120. <https://doi.org/10.1002/gdj3.109>.
- Noone, S., C. D’Arcy, S. Donegan, et al. 2024. “Investigating the Potential for Students to Contribute to Climate Data Rescue: Introducing the Climate Data Rescue Africa Project (CliDaR-Africa).” *Geoscience Data Journal* 11: 1–17. <https://doi.org/10.1002/gdj3.248>.
- Noone, S., C. Murphy, C. Coll, et al. 2015. “Homogenisation and Analysis of an Expanded Long-Term Monthly Rainfall Network for the Island of Ireland (1850–2010).” *International Journal of Climatology*. <https://doi.org/10.1002/joc.4522>.
- Peel, M. C., B. L. Finlayson, and T. A. McMahon. 2007. “Updated World Map of the Köppen-Geiger Climate Classification.” *Hydrology and Earth System Sciences* 11, no. 5: 1633–1644. <https://doi.org/10.5194/hess-11-1633-2007>.
- Petterssen, S. 1956. *Weather Analysis and Forecasting*. 2nd ed. McGraw-Hill.
- Python Software Foundation. 2023. “Python: Version 3.11 [computer program].” Accessed July 3, 2025. <https://www.python.org/>.
- Ralaingita, M. I., G. Ennis, J. Russell-Smith, K. Sangha, and T. Razanakoto. 2022. “The Kere of Madagascar: A Qualitative Exploration of Community Experiences and Perspectives.” *Ecology and Society* 27, no. 1: 1–17.
- Randriamarolaza, L. Y. A., E. Aguilar, O. Skrynyk, S. M. Vicente-Serrano, and F. Domínguez-Castro. 2022. “Indices for Daily Temperature and Precipitation in Madagascar, Based on Quality-Controlled and Homogenized Data, 1950–2018.” *International Journal of Climatology* 42, no. 1: 265–288. <https://doi.org/10.1002/joc.7243>.
- Redmond, K. T. 2002. “The Depiction of Drought.” *Bulletin of the American Meteorological Society* 83: 1143–1147. <https://www.jstor.org/stable/2621538>.
- Rennie, J. J., J. H. Lawrimore, B. E. Gleason, et al. 2014. “The International Surface Temperature Initiative Global Land Surface Databank: Monthly Temperature Data Release Description and Methods.” *Geoscience Data Journal* 1: 75–102. <https://doi.org/10.1002/gdj3.8>.
- Rigden, A., C. Golden, D. Chan, and P. Huybers. 2024. “Climate Change Linked to Drought in Southern Madagascar.” *npj Climate and Atmospheric Science* 7, no. 1: 41. <https://doi.org/10.1038/s41612-024-00583-8>.
- Ryan, C., C. Duffy, C. Broderick, et al. 2018. “Integrating Data Rescue Into the Classroom.” *Bulletin of the American Meteorological Society* 99, no. 9: 1757–1764. <https://journals.ametsoc.org/view/journals/bams/99/9/bams-d-17-0147.1.xm>.
- Saboureau, P. 1959. “Propos sur les cyclones et inondations à Madagascar en février et mars 1959.” *Bois et Forêts Des Tropiques* 67, no. 67: 3–12. <https://doi.org/10.19182/bft1959.67.a18747>.
- Schneider, U., A. Becker, P. Finger, A. Meyer-Christoffer, M. Ziese, and B. Rudolf. 2013. “GPCC’S New Land Surface Precipitation Climatology Based on Quality-Controlled in Situ Data and Its Role in Quantifying the Global Water Cycle.” *Theoretical and Applied Climatology* 115: 15–40. <https://doi.org/10.1007/s00704-013-0860-x>.
- Seneviratne, S. I., X. Zhang, M. Adnan, et al. 2021. “Weather and Climate Extreme Events in a Changing Climate.” In *Climate Change 2021: The Physical Science Basis. Contribution of Working Group I to the Sixth Assessment Report of the Intergovernmental Panel on Climate Change*, edited by V. Masson-Delmotte, P. Zhai, A. Pirani, et al., 1513–1766. Cambridge University Press. <https://doi.org/10.1017/9781009157896.013>.
- Serele, C., M. Kouadio, and F. Kayitakire. 2023. “Mitigating Proximate Impacts of Tropical Cyclone Landfalls in the Southwest Indian Ocean.” *Western Indian Ocean Journal of Marine Science* 22, no. 2: 147–161. <https://doi.org/10.4314/wiojms.v22i2.11>.
- Slivinski, L. C., G. P. Compo, J. S. Whitaker, et al. 2019. “Towards a More Reliable Historical Reanalysis: Improvements to the Twentieth Century Reanalysis System.” *Quarterly Journal of the Royal Meteorological Society* 145: 2876–2908.
- Tadross, M., L. Randriamarolaza, Z. Rabefitia, and K. Y. Zheng. 2008. *Climate Change in Madagascar: Recent Past and Future*. Vol. 18, 1771–1790. World Bank. Accessed August 15, 2025. <https://www.researchgate.net/publication/266244734>.
- Trewin, B., C. Earl-Spurr, and R. Cervený. 2024. “Tropical Cyclone Freddy: The World’s Longest-Lived Tropical Cyclone [in “State of the Climate in 2023”].” *Bulletin of the American Meteorological Society* 105, no. 8: S266. <https://doi.org/10.1175/BAMS-D-24-0098.1>.
- Trisos, C. H., I. O. Adekan, E. Totin, et al. 2022. “Africa.” In *Climate Change 2022: Impacts, Adaptation and Vulnerability. Contribution of Working Group II to the Sixth Assessment Report of the Intergovernmental Panel on Climate Change*, edited by H. O. Pörtner, D. C. Roberts, M. Tignor, et al., 1285–1455. Cambridge University Press. <https://doi.org/10.1017/9781009325844.011>.
- Van Loon, A. F. 2015. “Hydrological Drought Explained.” *WIREs Water* 2: 359–392. <https://doi.org/10.1002/wat2.1085>.
- Weiskopf, S. R., J. A. Cushing, T. L. Morelli, and B. J. Myers. 2021. “Climate Change Risks and Adaptation Options for Madagascar.” *Ecology and Society* 26, no. 4: 36. <https://doi.org/10.5751/ES-12816-260436>.
- Wilkinson, C., S. D. Woodruff, P. Brohan, et al. 2011. “Recovery of Logbooks and International Marine Data: The RECLAIM Project.”



*International Journal of Climatology* 31: 968–979. <https://doi.org/10.1002/joc.2102>.

World Bank. 2025b. “Madagascar—Climatology. Climate Change Knowledge Portal.” Accessed February 16, 2025. <https://climateknowledgeportal.worldbank.org/country/madagascar/climate-data-historical>.

World Meteorological Organization. 2012. “Standardized Precipitation Index User Guide (Svoboda M, Hayes M, Wood, D.).” WMO-No. 1090: Geneva.

World Meteorological Organization. 2016. “WMO Guidelines on Best Practices for Climate Data Rescue.” WMO-No. 1182. Accessed August 29, 2023. [https://library.wmo.int/doc\\_num.php?explnum\\_id=3318](https://library.wmo.int/doc_num.php?explnum_id=3318).